ESC European Society of Cardiology

European Heart Journal - Cardiovascular Imaging (2023) **00**, 1–17
https://doi.org/10.1093/ehjci/jead168

REVIEW

Tales from the future—nuclear cardio-oncology, from prediction to diagnosis and monitoring

Nidaa Mikail [1,2]*, Renata Chequer[3], Alessio Imperiale[4,5], Alexander Meisel[1,6], Susan Bengs [1,2], Angela Portmann[1,2], Alessia Gimelli [7], Ronny R. Buechel[1], Cathérine Gebhard[1,2,8], and Alexia Rossi[1,2]

[1]Department of Nuclear Medicine, University Hospital Zurich, Rämistrasse 100, 8091 Zurich, Switzerland; [2]Center for Molecular Cardiology, University of Zurich, Wagistrasse 12, 8952 Schlieren, Switzerland; [3]Department of Nuclear Medicine, Bichat University Hospital, AP-HP, University Diderot, 75018 Paris, France; [4]Nuclear Medicine, Institut de Cancérologie de Strasbourg Europe (ICANS), University Hospitals of Strasbourg, 67093 Strasbourg, France; [5]Molecular Imaging-DRHIM, IPHC, UMR 7178, CNRS/Unistra, 67093 Strasbourg, France; [6]Kantonsspital Glarus, Burgstrasse 99, 8750 Glarus, Switzerland; [7]Imaging Department, Fondazione CNR/Regione Toscana Gabriele Monasterio, Via G. Moruzzi 1, 56124 Pisa, Italy; and [8]Department of Cardiology, University Hospital Inselspital Bern, Freiburgstrasse 18, 3010 Bern, Switzerland

Received 25 April 2023; editorial decision 7 July 2023; online publish-ahead-of-print 19 July 2023

Cancer and cardiovascular diseases (CVD) often share common risk factors, and patients with CVD who develop cancer are at high risk of experiencing major adverse cardiovascular events. Additionally, cancer treatment can induce short- and long-term adverse cardiovascular events. Given the improvement in oncological patients' prognosis, the burden in this vulnerable population is slowly shifting towards increased cardiovascular mortality. Consequently, the field of cardio-oncology is steadily expanding, prompting the need for new markers to stratify and monitor the cardiovascular risk in oncological patients before, during, and after the completion of treatment. Advanced non-invasive cardiac imaging has raised great interest in the early detection of CVD and cardiotoxicity in oncological patients. Nuclear medicine has long been a pivotal exam to robustly assess and monitor the cardiac function of patients undergoing potentially cardiotoxic chemotherapies. In addition, recent radiotracers have shown great interest in the early detection of cancer-treatment-related cardiotoxicity. In this review, we summarize the current and emerging nuclear cardiology tools that can help identify cardiotoxicity and assess the cardiovascular risk in patients undergoing cancer treatments and discuss the specific role of nuclear cardiology alongside other non-invasive imaging techniques.

* Corresponding author. E-mail: nidaa.mikail@gmail.com

Graphical Abstract

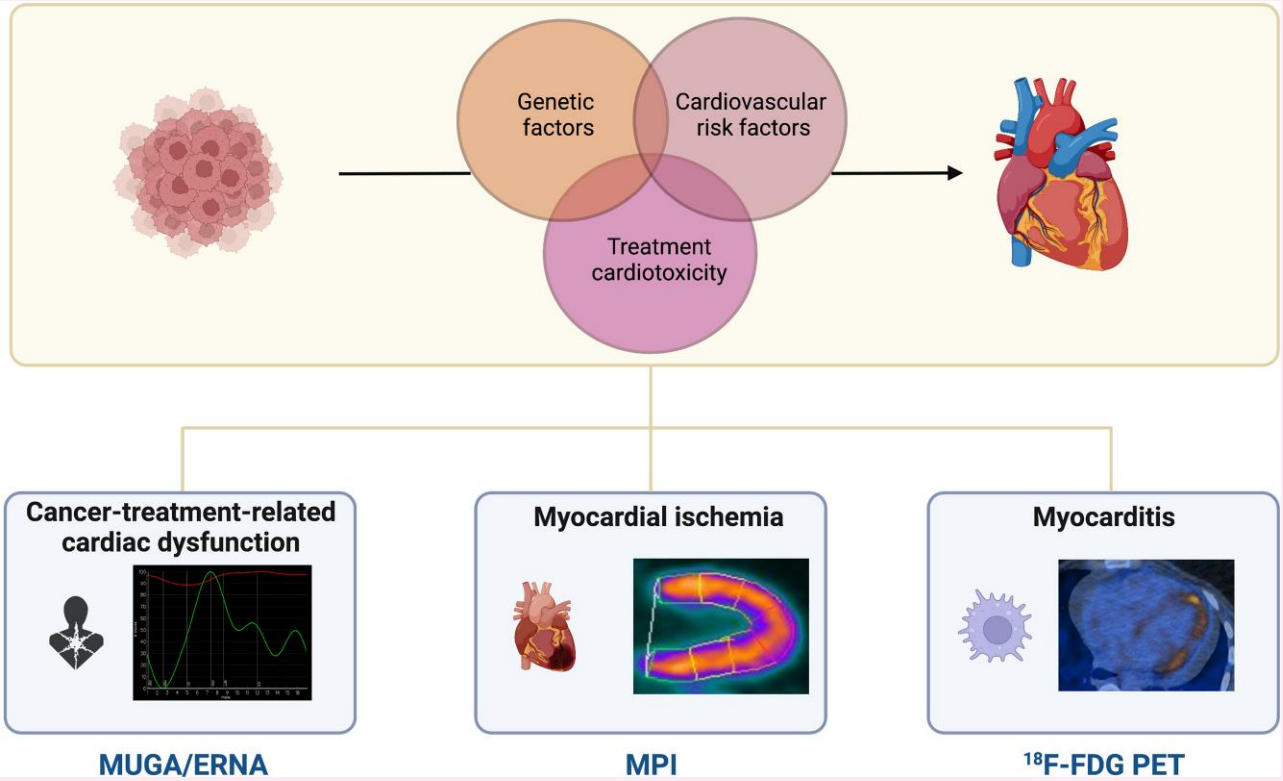

Pathophysiological pathways interconnecting cancers and CVD: genetic predispositions, cardiovascular risk factors, and cancer-treatment-related cardiotoxicity. CVD in cancer patients (and corresponding nuclear cardiology tools) consist mainly of cancer-treatment-related cardiac dysfunction (explored with MUGA/ERNA), myocardial ischaemia (with nuclear MPI), and myocarditis (with ^{18}F-FDG PET). Abbreviations: ^{18}F-FDG, fluor-18-radiolabelled fluorodeoxyglucose; CVD, cardiovascular diseases; ERNA, equilibrium radionuclide angiography; MPI, myocardial perfusion imaging; MUGA, multigated acquisition; PET, positron emission tomography.

Keywords cardio-oncology • nuclear cardiology • PET • scintigraphy • FDG • myocardial perfusion imaging • CMR • echocardiography • CTRCD

Introduction

Cancer and cardiovascular diseases (CVD), leading mortality causes in high-income countries,[1] are interconnected by common pathophysiological mechanisms[2] and risk factors.[3,4] Consequently, patients with cancer have an increased risk of CVD and major adverse cardiovascular events (MACE). Vice versa, cardiovascular risk factors (CVRFs) increase cancer risk.[5–7] Additionally, cancer treatments induce short- and long-term cardiotoxicity.[8,9] The prognostic improvement of oncological patients is slowly shifting their burden from cancer to cardiovascular mortality.[10] Hence, cardio-oncology is a steadily expanding field, as evidenced by the recent publication of the first European Society of Cardiology (ESC) cardio-oncology guidelines,[11] prompting the need for cardiovascular risk stratification markers in oncological patients.[12,13] Despite being challenged by echocardiography and cardiac magnetic resonance (CMR),[14] nuclear imaging remains a contemporary modality in patients receiving cardiotoxic therapies.

In this article, we briefly summarize the central mechanisms responsible for cancer-treatment-induced cardiotoxicity, review the main established and emergent nuclear cardiology tools useful in cancer settings, and discuss the role of nuclear medicine alongside echocardiography and CMR. Although also beneficial for managing cardiac tumours,[15,16] this review will not cover this topic.

Mechanisms of interaction between cancer and CVD

CVD and cancer are two sides of the same coin,[17] sharing identical pathophysiological pathways[18] (*Figure 1*).

Risk factors

Typical CVRFs include age, diabetes, hypertension, smoking, dyslipidaemia, and overweight,[19] all of which concomitantly increase cancer risk.[20] By promoting inflammation and oxidative stress, diabetes favours a pro-oncogenic environment.[21] Similarly, epidemiological data suggest a correlation between hypertension and dyslipidaemia on the one hand and cancer genesis on the other.[22] Smoking promotes atherosclerosis

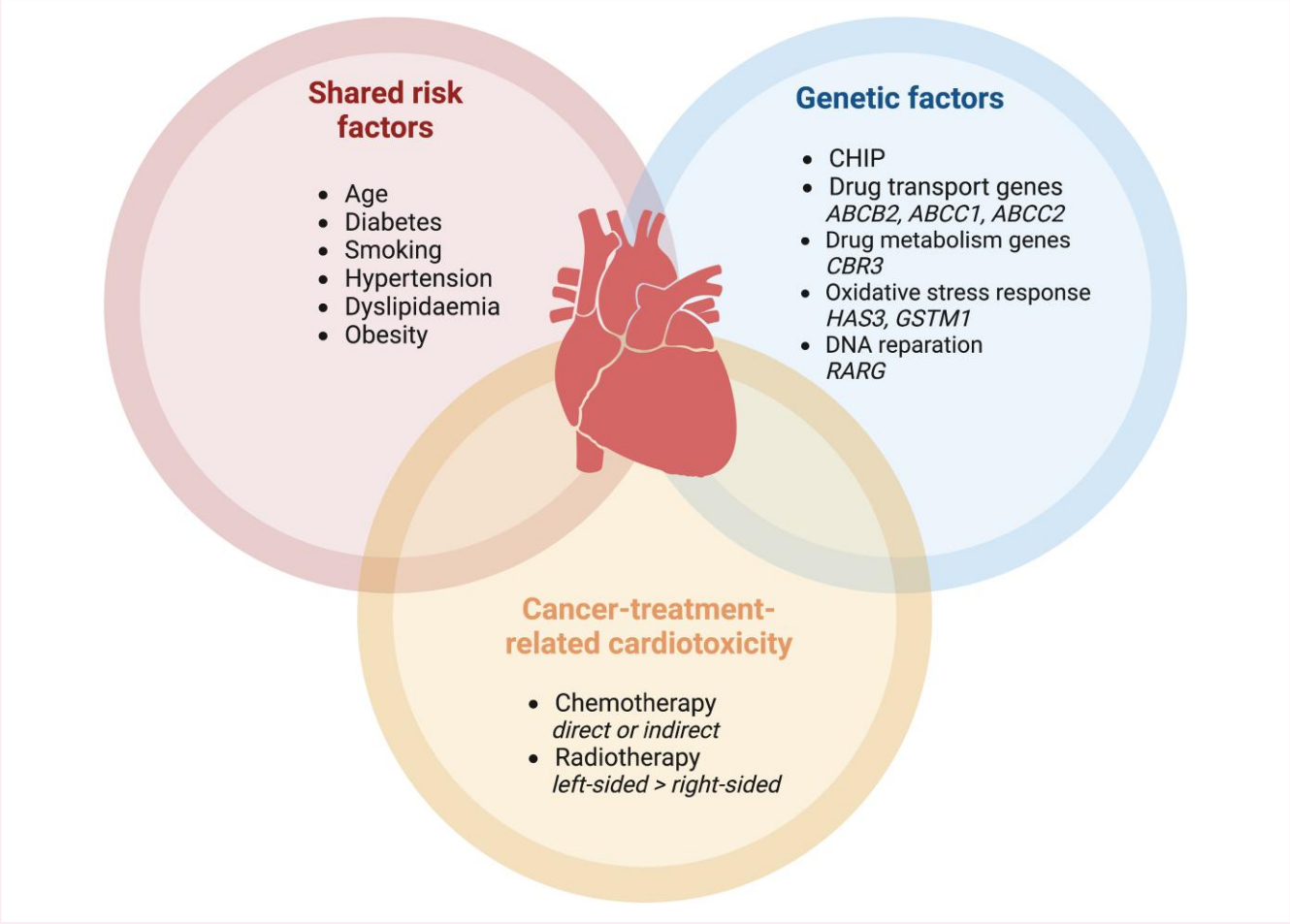

Figure 1 Mechanisms of CVD in cancer patients. Abbreviations: ABCB2, ABC transporter B family member 2 gene; ABCC1, ATP-binding cassette subfamily C member 1 gene; ABCC2, ATP-binding cassette subfamily C member 2 gene; CBR3, carbonyl reductase 3 gene; CHIP, clonal haematopoiesis of indeterminate potential; GSTM1, glutathione S-transferase mu 1 gene; HAS3, hyaluronan synthase 3 gene; RARG, retinoic acid receptor gene.

and cancer,[23,24] and a plethoric adipose tissue triggers oncogenic inflammatory molecules.[25]

Genetic factors

Intrinsic factors also predispose to CVD and cancer.[26] For instance, specific age-related somatic mutations, labelled clonal haematopoiesis of indeterminate potential (CHIP), increase the risk of haematological malignancy[27] and CVD.[28] Other genes involved in drug delivery and metabolism modulate the risk of cancer-therapy-induced cardiotoxicity,[26] either by increasing it, such as ATP-binding cassette transporters *ABCB4* and *ABCC*, or by decreasing it, for example, ATP-binding transporters (*ABCB1*) and solute carriers (*SLC28A3*).[26]

Cancer-treatment-related cardiotoxicity

Cancer-treatment-induced cardiotoxicity is a critical contributor to CVD[18] (*Table 1*). Cancer-treatment-related cardiac dysfunction (CTRCD), i.e. left ventricular (LV) dysfunction induced by cancer treatment, is the most common cardiotoxicity type.[8] Two types of CTRCD are distinguished.[29,30] Type I CTRCD, classically caused by anthracyclines, induces direct cumulative, dose-related, and usually irreversible cardiomyocyte damage. Type II CTRCD, traditionally induced by trastuzumab,[29] is a reversible and dose-independent myocardial dysfunction without structural alterations. Cancer treatment can also induce coronary artery disease (CAD), notably vasospasm and arterial thrombosis.[31,32] Likewise, chest radiotherapy favours atherosclerosis and fibrosis via inflammatory cascades in the coronary vessels.[6,33]

Lately, the introduction of immune checkpoint inhibitors (ICI) to the cancer armamentarium was accompanied by increasing reports of immune-related adverse events (IRAEs),[34,35] including myocarditis.[36]

Role of imaging for the early detection of CVD in cancer patients

The European Society for Medical Oncology guidelines highlight the need for an early screening of CVRFs and close cardiovascular monitoring of cancer patients.[13] This assessment includes a baseline evaluation of LV ejection fraction (LVEF) to guide the cancer treatment choice and the need for cardioprotective therapies.[13] However, LVEF alone can prove insufficient, since an LVEF drop is often a late-stage manifestation of cardiac damage.[37,38] Global longitudinal strain (GLS) assessment using echocardiography or CMR is a more sensitive marker of cardiac dysfunction and is, therefore, recommended.[14] Nonetheless, GLS is limited by scarce reproducibility,[39] prompting the need for alternative tools.

Table 1 Main types of cancer treatments and related toxic effects

Therapeutic class	Main treatment-induced toxicity mechanisms
Anthracyclines	Induction of oxidative stress, impaired autophagy, type II topoisomerase poisoning
Trastuzumab	Inhibition of epidermal growth factor receptor 2
Fluoropyrimidines	Induction of oxidative stress in cardiomyocytes, vasospasm by favouring endothelial and smooth cell dysfunction, coronary artery thrombosis
Platinum drugs	Induction of oxidative stress and of direct damage to cardiomyocytes and mitochondria, platelet aggregation
Taxanes	Direct cardiomyocyte and mitochondrial damage, alteration of cell division and microtubule dysfunction, oxidative stress, platelet aggregation, endothelial injury, haemorrhagic myopericarditis
Vascular endothelial growth factor (VEGF) inhibitors (tyrosine kinase inhibitors, monoclonal antibodies)	Arterial and venous thrombosis
Immune checkpoint inhibitors	Increased CD4 and CD8 lymphocyte infiltration inducing myopericarditis and arrhythmia
Radiotherapy	Coronary atherosclerosis and fibrosis by triggering acute and long-term coronary inflammation

Table 2 Main types of cancer-treatment-related cardiotoxicities and main cardiac cancers with the corresponding nuclear imaging diagnostic tools

	Type of toxicity/ disease	Most common toxic agents	Imaging tools	Comments
Cardiotoxicity	CTRCD	Anthracyclines, alkylating agents, TKI, proteasome inhibitors	MUGA (ERNA SPECT for RV function) ±First-pass ^{18}F-FDG PET	Diagnosis and monitoring of LV dysfunction
	Coronary artery disease	Alkylating-like agents, fluoropyrimidine (vasospasm) taxanes, radiotherapy, hormonotherapy (Arimidex, Aromasin, Femara)	SPECT MPI PET MPI	CACS derivable from hybrid CT imaging CMVD with PET MPI LVEF from SPECT and PET MPI
	Myocarditis	Alkylating agents, immune checkpoint inhibitors	^{18}F-FDG PET ±^{68}Ga-SSTR PET ±^{68}Ga-FAPI PET ±^{89}Zr-DFO-CD4 and ^{89}Zr-DFO-CD8a PET	Potential role for hybrid PET/CMR
Specific disease	Cardiac tumours	NA	^{18}F-FDG for aggressive primary tumours and NECs ^{68}Ga-SSTR for low-grade NETs	Diagnosis and staging

Abbreviations: ±, optional or used in research studies; ^{18}F-FDG, fluor-18-radiolabelled fluorodeoxyglucose; ^{68}Ga-FAPI, gallium-68-radiolabelled fibroblast activation protein inhibitors; ^{68}Ga-SSTR, gallium-68-radiolabelled somatostatin receptor; ^{89}Zr-DFO-CD4, zirconium-89-radiolabelled desferrioxamine-CD4; ^{89}Zr-DFO-CD8a, zirconium-89-radiolabelled desferrioxamine-CD8a; ^{99m}Tc, technetium-99m; ^{123}I-MIBG, iodine-123 metaiodobenzylguanidine; ATTR, transthyretin amyloidosis; CA, cardiac amyloidosis; CACS, coronary artery calcium score; CMVD, coronary microvascular dysfunction; CMR, cardiac magnetic resonance; CT, computed tomography; CTRCD, cancer-treatment-related cardiac dysfunction; ERNA, equilibrium radionuclide angiography; LVEF, left ventricular ejection fraction; MPI, myocardial perfusion imaging; MUGA, multigated acquisition; NA, not applicable; NEC, neuroendocrine carcinoma; NET, neuroendocrine tumour; PET, positron emission tomography; SPECT, single-photon emission computed tomography; TKI, tyrosine kinase inhibitors.

Nuclear medicine imaging and particularly multigated acquisition (MUGA) scintigraphy have historically been at the frontline of LV monitoring in oncological patients.[40,41] Although challenged by CMR,[42] nuclear cardiology provides critical information for diagnosing, monitoring, and risk-stratifying cancer patients[15,16,43–45] (*Table 2*). In the following part, we will review how nuclear cardiology can detect cardiac complications in oncological patients and discuss its role alongside echocardiography and CMR.

Diagnosis of cancer-treatment-related toxicity

CTRCD and LV systolic dysfunction

The ESC defines CTRCD as (i) a ≥10% LVEF decrease from baseline to below 50%, (ii) with a GLS drop of ≥15% from baseline, confirmed by a 2–3-week repeat study, in the context of cancer treatment.[14] While

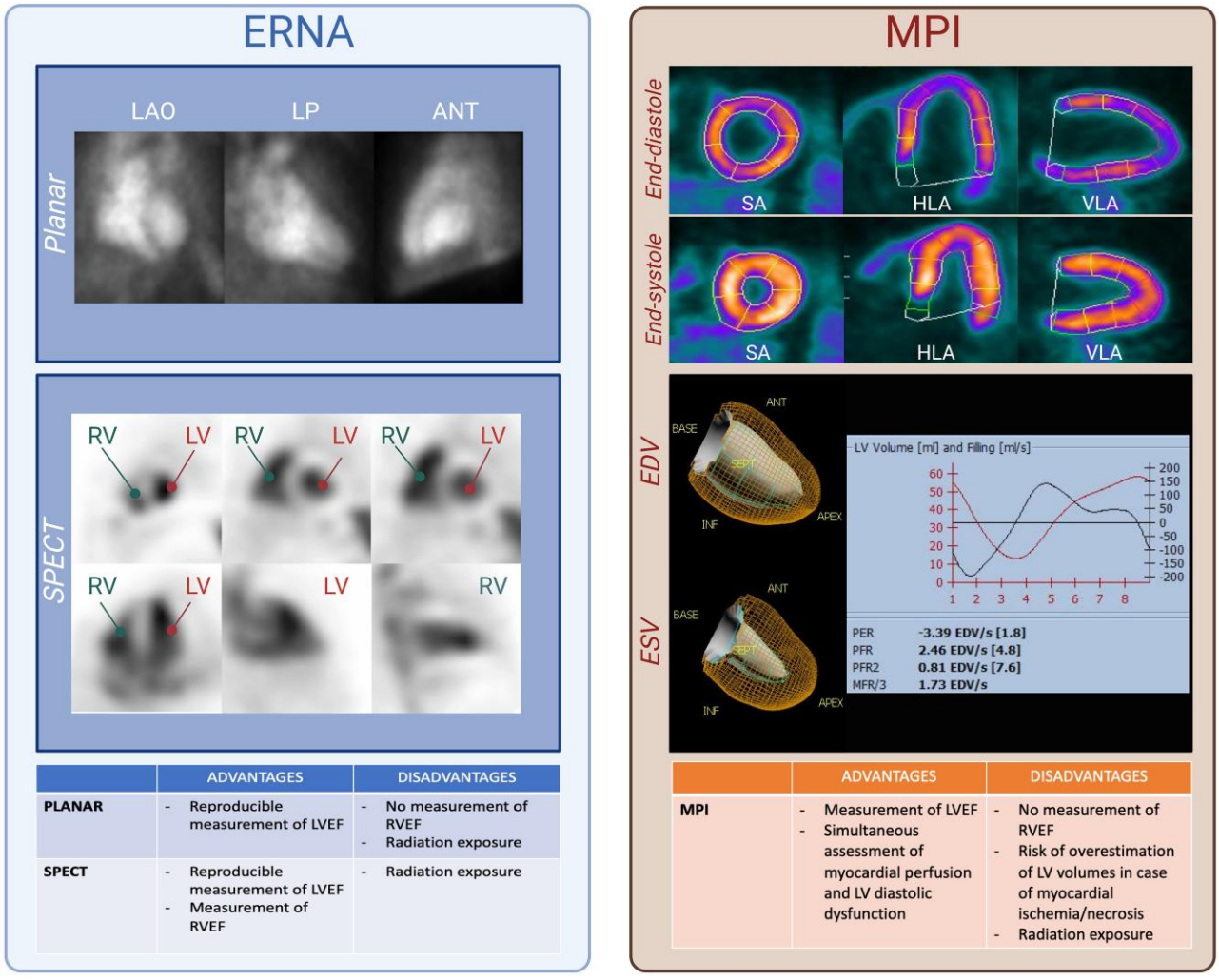

	ADVANTAGES	DISADVANTAGES
PLANAR	- Reproducible measurement of LVEF	- No measurement of RVEF - Radiation exposure
SPECT	- Reproducible measurement of LVEF - Measurement of RVEF	- Radiation exposure

	ADVANTAGES	DISADVANTAGES
MPI	- Measurement of LVEF - Simultaneous assessment of myocardial perfusion and LV diastolic dysfunction	- No measurement of RVEF - Risk of overestimation of LV volumes in case of myocardial ischemia/necrosis - Radiation exposure

Figure 2 LV function assessment with nuclear cardiology. *Left panel*: ERNA techniques for LVEF assessment based on radiolabelled erythrocytes' activity. Planar ERNA: end-diastolic and end-systolic LV volumes derived from LAO projections. Additional incidences include LP and anterior projections. SPECT ERNA: 3D reconstructions allowing LVEF/RVEF measurement. *Right panel*: NH_3 PET MPI during end-diastole and end-systole enabling EDV/ESV estimation. Accurate volume measurement with MPI necessitates preserved myocardial perfusion. Diastolic (D) function can also be studied. Abbreviations: ANT, anterior; CHIP, clonal haematopoiesis of indeterminate potential; EDV, end-diastolic volume; ERNA, equilibrium radionuclide angiography; ESV, end-systolic volume; HLA, horizontal long axis; LAO, left anterior oblique; LP, left profile; LV, left ventricle; LVEF, left ventricular ejection fraction; MFR, mean filling rate during the first third of diastole; mL, millilitres; mL/s, millilitres per second; MPI, myocardial perfusion imaging; PER, peak ejection rate; NH_3, ammonium; PET, positron emission tomography; PFR, peak filling rate; PFR/2, peak filling rate during the first half of diastole; RV, right ventricle; RVEF, right ventricular ejection fraction; SA, short axis; SPECT, single-photon emission computed tomography; VLA, vertical long axis.

only echocardiography and CMR can estimate GLS,[46] MUGA robustly determines LVEF.[47,48] In MUGA, cardiac volumes are derived from heart-centred images of the patient's own radiolabelled erythrocytes[49] and are therefore not influenced by geometric assumptions about the myocardial wall.[50] Three types of MUGA are distinguished: (i) first-pass MUGA, (ii) planar equilibrium radionuclide angiography (ERNA), and (iii) single-photon emission computed tomography (SPECT) ERNA. In practice, first-pass MUGA is limited to specific indications [right ventricular ejection fraction (RVEF) and shunt assessment[49,51]], and only ERNA is used to assess CTRCD. Planar ERNA is acquired when the radiotracer has reached equilibrium and allows measuring LVEF[52] (*Figure 2*), not RVEF, because of the superposition of heart structures. However, ERNA can also be performed with three-dimensional (3D) gated SPECT, which enables the delineation of both LVEF and RVEF.[49,53–56] Overall, MUGA displays a high inter- and intra-observer reproducibility for LVEF measurement,[57] which is crucial for serial follow-up during anticancer treatment.[14,58] MUGA also helps select patients who can safely tolerate higher cumulative anthracycline doses, i.e. asymptomatic patients with LVEF > 40% and a drop in LVEF < 10%,[13,41] significantly reducing heart failure occurrence.[59] Although in good agreement,[60] LVEF tends to be higher with SPECT than with planar ERNA,[61] which needs to be taken into consideration for

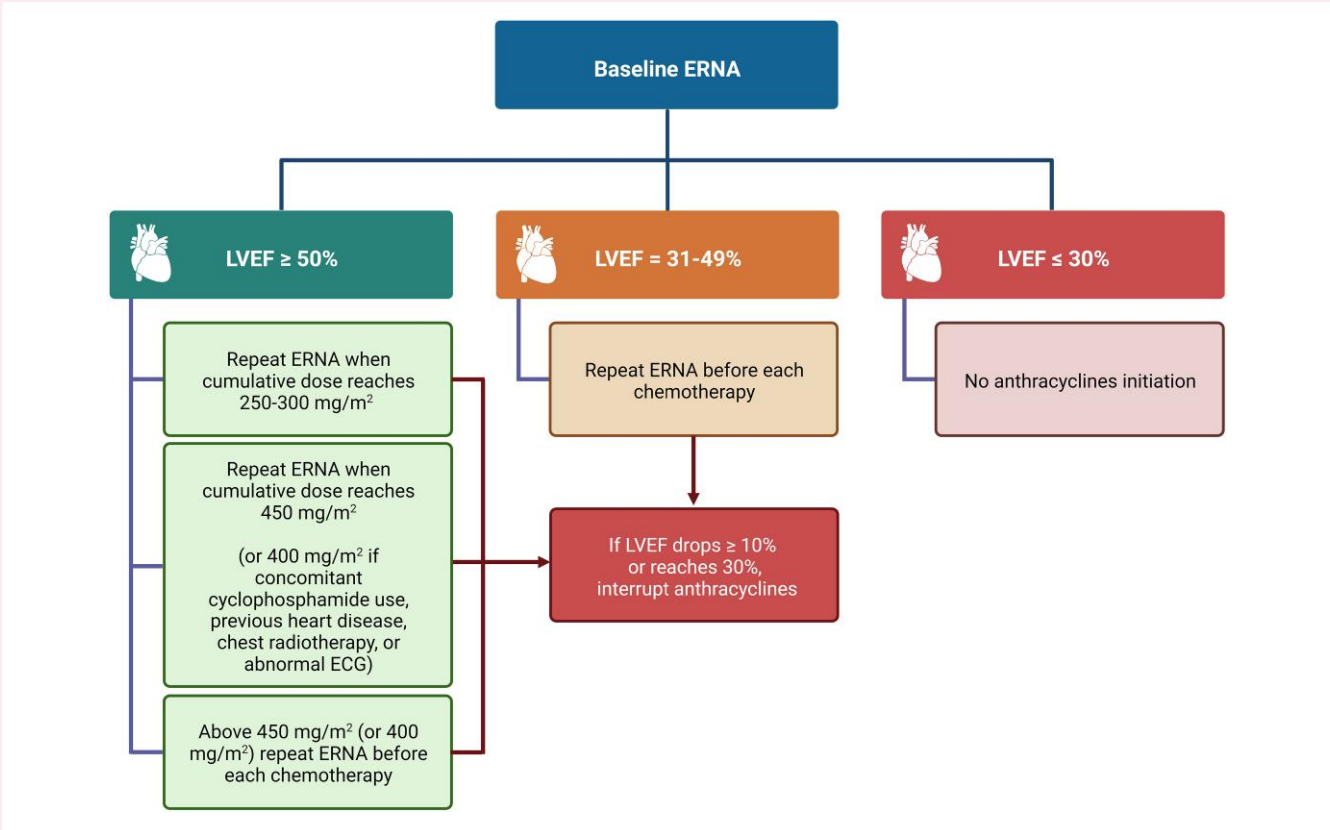

Figure 3 SNMMI/EANM Guidelines for ERNA-based LVEF monitoring in anthracycline-treated patients. Abbreviations: EANM, European Association of Nuclear Medicine; ECG, electrocardiogram; ERNA, equilibrium radionuclide angiography; LVEF, left ventricular ejection fraction; SNMMI, Society of Nuclear Medicine and Molecular Imaging.

monitoring.[14] Similarly, in breast cancer patients, MUGA gives slightly lower LVEF values than CMR.[62] As such, when using MUGA, for an LVEF threshold of 50%, this difference could result in 35% more patients being diagnosed with CTRCD than with CMR.[62] Hence, given that LV volumes tend to shrink and LVEF to increase after menopause,[63] CTRCD thresholds might need to be adapted in women.[64] Regarding surveillance, the European and American nuclear medicine societies recently issued an expert consensus for monitoring LVEF by ERNA for patients receiving anthracyclines,[65] which has been summarized in *Figure 3*.

A major drawback of MUGA is radiation exposure. Indeed, MUGA requires the injection of 555–1110 MBq (7–15 MBq/kg in children) of radiotracers,[65] which in case of serial follow-up increases theoretically (albeit minimally) cancer risk.[66–68] Cadmium-zinc-telluride (CZT)-based cameras, which detectors are more sensitive than conventional sodium iodide (NaI) ones, enable a two- to three-fold reduction in injected activity without altering image quality,[60,69,70] hence decreasing the radiation burden. CZT-derived LVEF highly correlates with the one obtained from planar NaI detectors.[71] CZT-based SPECT ERNA is also in high agreement with CMR for RVEF.[72] Interestingly, LVEF can be obtained from fluor-18-radiolabelled fluorodeoxyglucose positron emission tomography (^{18}F-FDG PET) gated first-pass acquisitions, showing excellent concordance with planar ERNA.[73] Given that ^{18}F-FDG PET is the mainstay for cancer staging, this elegant approach allows simultaneously measuring LVEF with no additional radiation exposure. However, first-pass cardiac ^{18}F-FDG acquisitions result in a prolonged acquisition time (5 min), reducing the available scanning time for other patients.

In practice, MUGA has long been supplanted by the more readily available and non-irradiating echocardiography and CMR (*Figure 4*). Transthoracic echocardiography (TTE) is the frontline risk stratification exam, owing to its wide availability, harmfulness, ability to assess morphology (including valves), function, and GLS. Whenever available, 3D echocardiography is preferred over 2D, given its higher reproducibility for LVEF and GLS assessment.[74–76] GLS detects early signs of systolic dysfunction before any LVEF drop, with a change in GLS $\geq$ 15% predicting the risk of CTRCD.[46] Importantly, a GLS-based cardioprotective strategy reduces the rate of CTRCD in patients undergoing anthracycline.[77] Nonetheless, echography strain measurements lack inter-device standardization, which limits their routine use.[78] In case of reduced acoustic window or low image quality, CMR is recommended as a second-line technique.[11,75] CMR is considered the reference exam to calculate cardiac volumes and function and can detect even minor LVEF impairments and volume changes.[75] The latter is particularly important in patients undergoing anticancer treatments, in whom CTRCD can manifest as an isolated LV end-diastolic volume reduction.[79] Moreover, CMR accurately determines RVEF, which can be asymptomatically reduced in cancer survivors.[80] Besides volumes and strain assessment, CMR is a promising tool for the early detection of cancer-treatment-related myocardial oedema and fibrosis via T1/T2 mapping and extracellular volume (ECV) measurement.[81] Increased T1/T2 relaxation times hold promise to predict subsequent CTRCD,[81] although there is a significant overlap between mapping parameters of patients who develop CTRCD and those who do not.[82]

During cancer treatment, echocardiography is the preferred modality for monitoring cardiac function.[14] Surveillance frequency depends

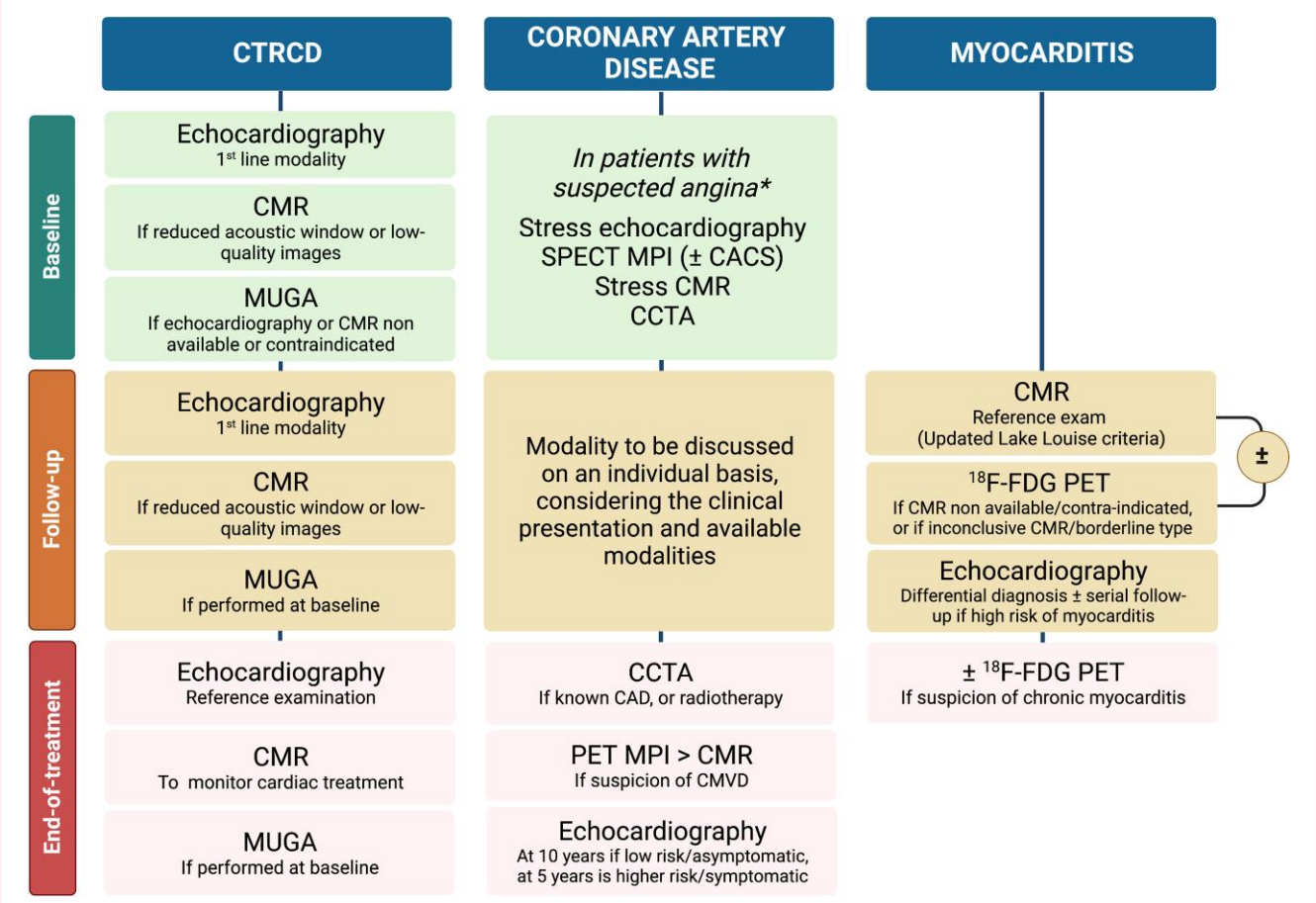

Figure 4 Algorithm proposal for non-invasive imaging in patients undergoing anticancer treatment. Abbreviations: ^{18}F-FDG, fluor-18-radiolabelled fluorodeoxyglucose; CACS, coronary artery calcium score; CAD, coronary artery disease; CCTA, coronary computed tomography angiography; CMR, cardiac magnetic resonance; CTRCD, cancer-treatment-related cardiac dysfunction; LVEF, left ventricular ejection fraction; SNMMI, Society of Nuclear Medicine and Molecular Imaging; MPI, myocardial perfusion imaging; MUGA, multigated acquisition; PET, positron emission tomography; SPECT, single-photon emission computed tomography. *The choice of imaging modality should be based on symptoms, known CAD, pretest probability, local availability and expertise, and patient characteristics.

on a cardiotoxicity risk profile based on patient- and treatment-related factors.[14] Importantly, given the inter-imaging variability, it is crucial to perform follow-up using the same modality.[83] Indeed, minor LVEF variations are essential to detect, as they could be an early sign of cardiac toxicity. Compared with CMR, 2D and 3D TTE tend to underestimate LV volumes.[84] Similarly, limits of agreement between MUGA and CMR often exceed ±10%,[48] which could lead to incorrectly classifying patients with CTRCD. In this regard, MUGA's radiation exposure argues against its systematic use for the follow-up of patients undergoing anticancer treatment.

After the end of treatment, patients who developed CTRCD should be monitored using echocardiography. In patients in whom a cardiac medication was introduced to mitigate treatment side effects, CMR is an option to assess treatment response.[14]

In summary, the 2022 ESC Guidelines on cardio-oncology only recommend MUGA as a third-line technique to assess LVEF, i.e. if TTE and CMR are unavailable or in case of CMR contraindication.[11,14] Of note, the guidelines mention the potential interest of assessing the myocardial ^{18}F-FDG uptake during intercourse PET/computed tomography (CT), as its increase could indicate an LVEF decline[85] and, therefore, trigger LVEF assessment.[14]

Coronary artery disease

Cancer is a prothrombotic condition associated with enhanced platelet reactivity and circulating procoagulant products, which increase the atherosclerotic burden.[86] Additionally, cancer treatments themselves (particularly chest radiotherapy) induce endothelial injuries, favouring vasospasm and thrombosis.[87–89] Hence, screening for ischaemic heart diseases (IHD) is recommended in patients with intermediate-to-high pre-test likelihood[46] undergoing heart-damaging cancer therapy,[8] especially anthracyclines and chest radiotherapy.[90,91] Such screening can be done with SPECT myocardial perfusion imaging (MPI), a mainstay in this indication.[92]

SPECT myocardial perfusion abnormalities can appear either during radiotherapy[93] or later, up to 20 years after treatment completion.[94] Most perfusion abnormalities develop in the apical territory,[89,95] indicating left anterior descending artery damage.[96,97] Accordingly, myocardial perfusion impairment is more prevalent in left-sided than right-sided chest cancer,[89,98] a risk that linearly correlates with cardiac exposure volume.[94,99] In patients with left-sided breast cancer, an irradiated cardiac volume of >5% is associated with significantly higher rates of perfusion abnormalities than with lower volumes.[100] Interestingly, in cancer patients, SPECT-detected myocardial ischaemia does not correlate well with underlying obstructive CAD,[97] highlighting

the importance of coronary microvascular dysfunction (CMVD) and coronary spasm in this population.[101–103]

PET MPI is the reference non-invasive modality to diagnose CMVD, using ^{13}N-ammonia (^{13}N-NH_3), ^{82}Rubidium (^{82}Rb), and ^{15}O-water (^{15}O-H_2O) radiotracers.[104] PET MPI allows for measuring myocardial blood flow (MBF) and coronary flow reserve (CFR), which are central to CMVD diagnosis.[105] In patients undergoing chest radiotherapy, PET MPI shows an inverse correlation between the mean radiation dose to the heart and CMVD.[106,107] Moreover, MBF could have prognostic value, with low CFR values being associated with an increased cumulative incidence of MACE in breast cancer patients.[108]

Another prognostic parameter is the coronary artery calcium score (CACS). CACS is obtained from a non-enhanced CT and quantifies the degree of coronary artery calcification, expressed with the Agatston score.[109] CACS = 0 in asymptomatic patients is associated with a very low prevalence of severe coronary stenosis and high-risk plaque features.[110] Conversely, an Agatston score of >400 is predictive of MACE, even for normal MPI.[111] CACS can easily be yielded from the low-dose CT of PET/CT and SPECT/CT cameras, showing high agreement with the one obtained from standard non-enhanced scans.[112–114] Since ^{18}F-FDG PET/CT is part of routine oncological work-up, cardiovascular risk stratification with CACS could simultaneously be performed without additional radiation or cost.[115]

Beyond myocardial perfusion, nuclear MPI can also estimate LVEF[116,117] (*Figure 2*). However, contrary to MUGA, MPI indirectly estimates cardiac volumes based on myocardial wall motion. In case of infarction, the necrotic segment is devoid of signal, leading to overestimating LV volumes.[118] Another limitation of SPECT MPI is its inability to assess RVEF. Although more accurate,[119–121] CZT cameras give lower values than conventional SPECT cameras,[122] stressing the importance of performing serial follow-up using the same modality.

Nuclear MPI is only one of the tools available for myocardial ischaemia screening alongside stress echocardiography, and CMR. Additionally, contrast-enhanced coronary computed tomography angiography (CCTA) is an alternate tool which provides information on coronary plaque burden and coronary stenosis assessment.[11,14] Although the recent European guidelines on cardio-oncology do not give strict recommendations on which modality to prefer in which setting,[11] echocardiography and CMR remain the frontline techniques in this setting.[14] Overall, three scenarios can be distinguished: baseline screening, follow-up during treatment, and end-of-treatment surveillance[14] (*Figure 4*).

Baseline screening should always be considered in the oncological population, given their increased CAD risk.[14] CACS assessment is an easy and minimally invasive way of characterizing the baseline CAD risk. If CACS = 0, the risk of dying from CAD within 5 years of cancer diagnosis remains below the mortality risk from cancer itself; conversely, if CACS > 300, the 5-year CAD mortality risk exceeds the cancer mortality risk,[123] prompting more aggressive management.[14] As abovementioned, CACS can be extracted from ^{18}F-FDG PET's low-dose CT without additional scanning time, cost, or radiation.[115] As the mainstay baseline staging exam of most cancer types, ^{18}F-FDG-PET-based CACS appears as a reasonable option for baseline CAD risk assessment. Advanced explorations should be preferred in patients with a higher baseline CAD risk. In nononcological settings, non-enhanced CT and CCTA are the first-line exam for detecting coronary calcifications and coronary stenosis in patients with low-to-intermediate CAD risk.[92] Given the increased CAD risk in oncological patients, detection of coronary stenosis using CCTA can be discussed in symptomatic patients with no CAD history.[14] However, this comes at the expense of increased radiation exposure.[124] Stress echocardiography is indicated in patients with intermediate-to-high CAD probability undergoing ischaemia-inducing chemotherapies, such as fluorouracil, bevacizumab, sorafenib, and sunitinib.[125] In addition to ischaemia, stress echocardiography could unveil patients at risk of developing CTRCD,[126,127] a 5-unit fall in LV contractile reserve during dobutamine echocardiography predicting the subsequent LVEF drop.[128] Myocardial perfusion CMR imaging using pharmacological stress is also an option, but its use for systematic screening is conflicted by its relatively low availability.[14] SPECT MPI is a well-validated and widely accessible modality that additionally provides CACS in case of hybrid SPECT/CT.[113]

During treatment, there is no clear recommendation as to which modality to prioritize and the exploration frequency, which will depend on the clinical presentation and the available modalities.

After treatment completion, CCTA is an option for CAD identification,[14] particularly in patients with known CAD, whose plaque progression can be accelerated by anticancer treatment, and in young patients treated with chest radiotherapy, i.e. at risk of perivascular fibrosis.[14,90] Radiotherapy can also induce valve leaflet calcification, which can be assessed by CT.[90] A limitation of CCTA is for the routine detection of microvascular dysfunction, although dynamic CT MPI is promising in this regard.[129–132] Conversely, CMR detects both segmental ischaemia and CMVD,[133] with the advantage over nuclear MPI of being devoid of radiation exposure. Still, CMR assessment of MBF remains in the research realm,[134] and PET MPI is the reference exam for CMVD,[104] displaying higher accuracy, reproducibility, and prognostic value than CMR.[135,136] This favours PET in patients at risk of CMVD, particularly women with breast cancer[108,137] and patients who underwent chest radiotherapy.[106,138]

Myocarditis

The last years have witnessed the development of immunotherapy, a new class of anticancer treatment that leverages the immune system to harness cancer progression. The primarily used class of immunotherapy is ICI. Immune checkpoints are T-lymphocyte-expressed receptors that recognize ligands at the surface of normal cells. The receptor–ligand binding inhibits the T-cell, preventing it from targeting normal cells.[139] Some cancer cells express immune-checkpoint-binding ligands and can thus trick and inhibit T-lymphocytes. ICI block the receptor–ligand bond, allowing T-cells to recognize and attack cancer cells.[139] The downfall of lifting T-cell inhibition is that this may unleash IRAEs.[140] Cardiovascular IRAEs occur with an incidence ranging from 1.14 to 5%[140] and include notably myocarditis, pericarditis, vasculitis, and Takotsubo cardiomyopathy.[141,142]

Diagnosing ICI-related myocarditis is challenging because of the various presentations[143] and the prolonged interval between drug administration and symptom onset.[140] While CMR is the reference exam,[144] PET can also orient the diagnosis. Due to its availability and high uptake in inflammatory cells, ^{18}F-FDG is a natural candidate in this indication,[145] classically displaying focal or diffuse patchy myocardial ^{18}F-FDG uptake with no vascular systematization[146] (*Figure 5*). Despite a good spatial agreement between ^{18}F-FDG uptake and T2 hyperintensity/late gadolinium enhancement (LGE), the diagnostic accuracy of ^{18}F-FDG PET/CT in myocarditis is low.[148] Several factors might explain this, such as an inadequate high-fat/low-carbohydrate diet, the initiation of immunosuppressive treatment, and the delay between myocarditis onset and image acquisition. Acquisition timing is indeed critical, with a small series showing a 100% sensitivity when ^{18}F-FDG PET was performed within 14 days of disease onset vs. 20% when performed later.[146] In 2019, Bonaca *et al.*[147] proposed a definition of ICI-related myocarditis that includes ^{18}F-FDG PET, with myocarditis deemed as *possible* in any 'scenario meeting criteria for possible myocarditis (i.e. not explained by any other diagnosis such as acute coronary syndrome, trauma or Takotsubo cardiomyopathy on CMR, ultrasound, and cardiac biomarkers) with ^{18}F-FDG PET showing patchy cardiac ^{18}F-FDG uptake without another explanation'.

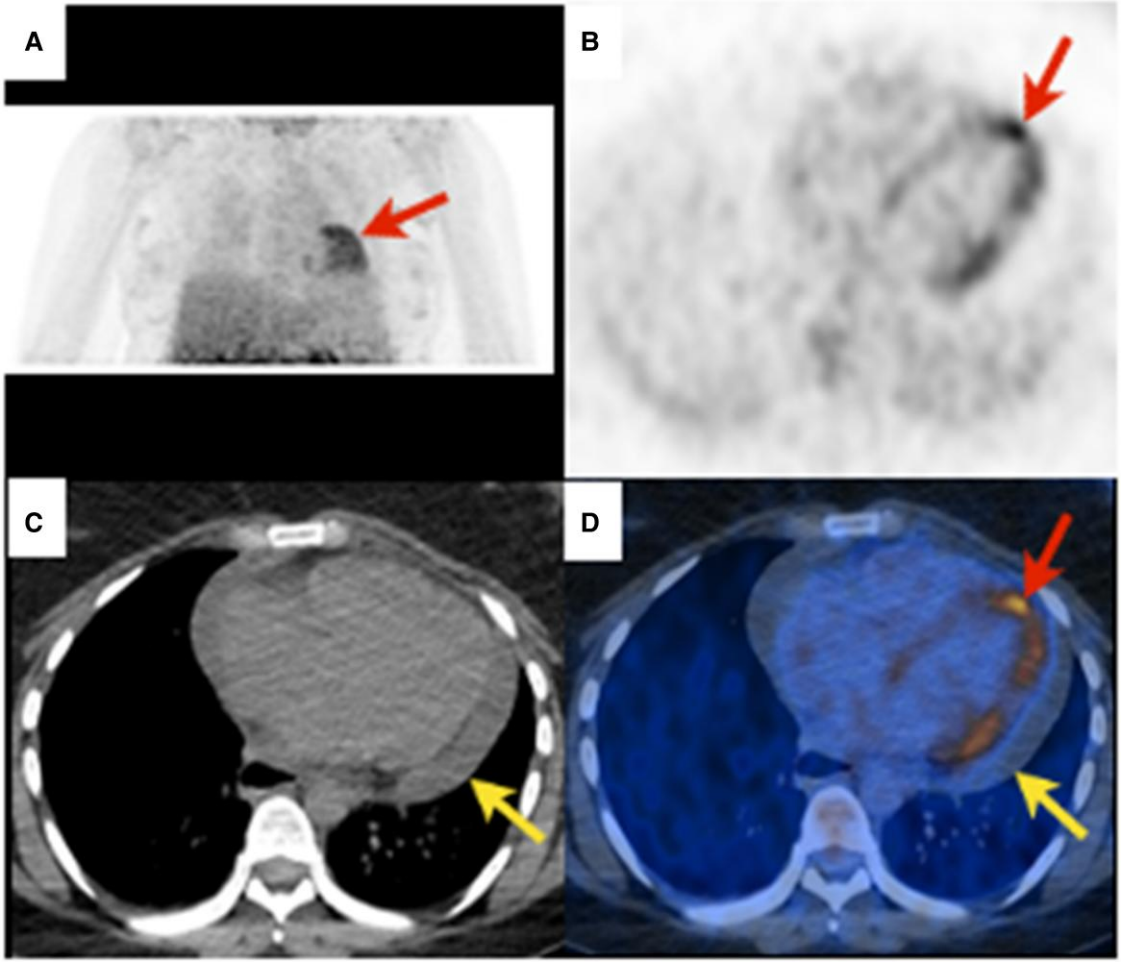

Figure 5 Myocarditis. Twenty-seven-year-old dyspnoeic woman with widespread concave ST elevation on ECG and increased C-reactive protein (131 mg/L, $N < 4$), suggestive of myocarditis. ^{18}F-FDG PET revealing diffuse heterogeneous ('patchy') myocardial ^{18}F-FDG uptake [red arrows, (*A*) maximal intensity projection, (*B*), and (*D*) axial slices]. Non-enhanced CT showing pericardial effusion [(*C*), yellow arrow] without ^{18}F-FDG uptake [(*D*), yellow arrow] related to pericarditis. According to the Bonaca *et al.*[147] criteria, *possible myocarditis* was retained.

Other promising radiotracers target somatostatin receptors (SSTRs) overexpressed at the surface of vascular macrophages.[149] The lower albeit variable[150] physiologic myocardial uptake of SSTR radiotracers reduces the risk of false positives. In a small population of nine patients, gallium-68-radiolabelled DOTA0-D-Phe1-Tyr3-octreotide (^{68}Ga-DOTATOC) PET/CT had a 100% sensitivity to diagnose ICI-related myocarditis, despite the initiation of steroid and immunosuppressive therapy.[151] Recently, a ^{68}Ga-radiolabelled tracer targeting fibroblast activation protein inhibitors (^{68}Ga-FAPI) was introduced in oncological diseases.[152,153] In three patients fulfilling the Bonaca *et al.*[147] criteria for definite ICI-related myocarditis, focal myocardial uptake of ^{68}Ga-FAPI identified cardiac remodelling territories.[154] Similarly, the upregulation of translocator protein-18 kDa (TSPO) and chemokine receptors types 4 and 12 in inflammatory cells suggests a role for radiolabelled TSPO and ^{68}Ga-pentixafor in myocarditis,[155,156] although dedicated studies still need to be performed. Along the same line, radiotracers targeting the C-X-C motif chemokine receptor 4 overexpressed by leucocytes represent an exciting approach to diagnosing myocardial inflammation.[157] Finally, novel inflammation radiotracers targeting CD4 and CD8 cells, zirconium-89-radiolabelled desferrioxamine-CD4 (^{89}Zr-DFO-CD4) and ^{89}Zr-DFO-CD8a, are under investigation and hold the potential to image myocarditis.[158] Their high specificity could prove particularly useful in ICI-related myocarditis. Indeed, the reference treatment for myocarditis is steroids, which alleviate the antitumour effect of ICI.[159] Therefore, establishing the diagnosis with certainty might reduce unnecessary immunosuppressive therapies or withholding ICI.

In practice, however, the guidelines recommend echocardiography and CMR as first-line examinations in suspected ICI-associated myocarditis and recommend cardiac PET only if CMR is non-available or contraindicated[11] (*Figure 4*). Echocardiography's primary role is to rule out non-inflammatory cardiac diseases and serve as a reference exam for LVEF monitoring.[160] Serial echocardiography could also be discussed in patients at high risk of myocarditis, i.e. patients undergoing a combination of ICI, ICI with another cardiotoxic regimen, or in case of pre-existing CVD.[14] The mainstay examination for diagnosing myocarditis remains CMR, using the Lake Louise criteria,[161] updated in 2018 with the implementation of mapping techniques.[160] The Lake Louise criteria consist of a triad combining oedema (as assessed by T2-weighted acquisitions), hyperaemia [reflected by early gadolinium enhancement (EGE)], and necrosis (set by LGE). The presence of ≥2 out of 3 criteria in a suggestive context establishes the diagnosis of myocarditis with high sensitivity and specificity.[144] Mapping techniques improve intra-

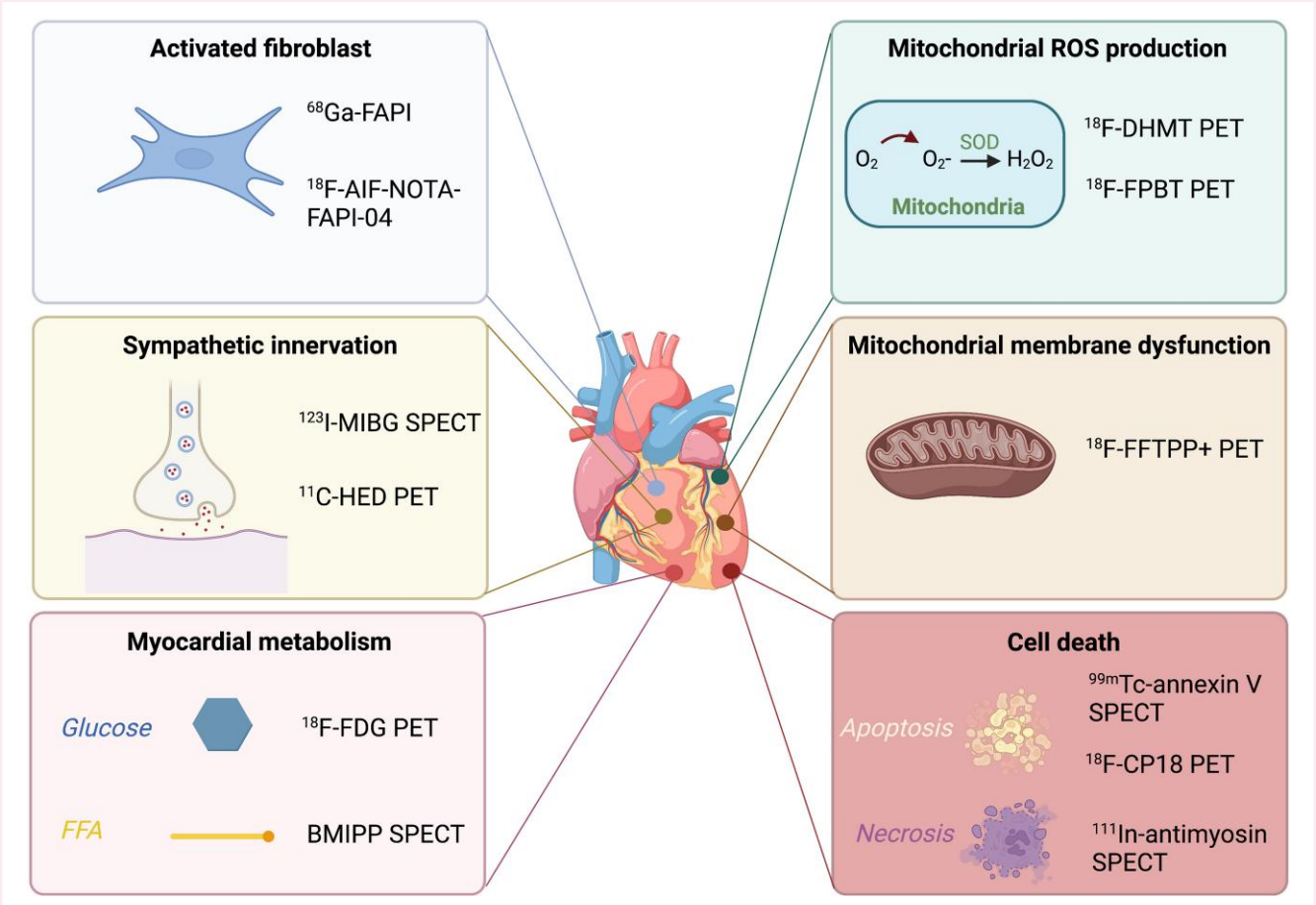

Figure 6 Main metabolic targets of early cardiac toxicity and corresponding radiotracers. Abbreviations: ^{11}C-HED, carbon-11-radiolabelled hydroxyephedrine; ^{18}F-AIF-NOTA-FAPI-04, fluor-18-labelled 1,4,7-triazacyclononane-N,N′,N″-triacetic acid-conjugated FAP inhibitor 04; ^{18}F-CP18, fluor-18-radiolabelled caspase 3 substrate; ^{18}F-DHMT, fluor-18-radiolabelled 6-(4-((1-(2-fluoroethyl)-1H-1,2,3-triazol-4-yl)methoxy) phenyl)-5-methyl-5,6-dihydrophenanthridine-3,8-diamine; ^{18}F-FDG, fluor-18-radiolabelled fluorodeoxyglucose; ^{18}F-FTPP+, fluor-18-radiolabelled (4-fluorophenyl)triphenylphosphonium; ^{18}F-FPBT, fluor-18-radiolabelled 3-(3-fluoropropyl)-2-phenyl-2,3-dihydrobenzo[d]thiazole; ^{68}Ga-FAPI, gallium-68-radiolabelled fibroblast activation protein inhibitor; ^{99m}Tc, technetium-99m; ^{111}In, indium-111; ^{123}I-MIBG, iodine-123 metaiodobenzylguanidine; BMIPP, beta-methyl-iodine-123 phenylpentadecanoic acid; H_2O_2, hydrogen peroxide; O_2, oxygen; O_2-, ion oxide; PET, positron emission tomography; ROS, reactive oxygen species; SOD, superoxide dismutase; SPECT, single-photon emission computed tomography.

and inter-observer diagnostic confidence, the specificity for detecting active inflamamtion and edema, and improve the detection of milder forms of myocarditis.[160] Additionally, reduced GLS and global circumferential strain could help risk-stratify patients with ICI myocarditis, the magnitude of strain reduction being predictive of MACE.[162] Nonetheless, the updated Lake Louise criteria might not be as performant in ICI myocarditis. Indeed, recent data show the sensitivity of CMR to be lower in the latter, possibly because of reduced LGE in the early phase.[163,164] Detecting LGE is particularly challenging in borderline forms of myocarditis,[165] which display less necrotic insult and patchy distribution. Such patients might benefit from ^{18}F-FDG PET, given the increased ^{18}F-FDG uptake in myocarditis areas devoid of LGE, which could also guide potential myocardial biopsies.[148] However, no dedicated study has assessed the diagnostic performance of ^{18}F-FDG PET in this specific subgroup. ^{18}F-FDG PET could also help distinguish chronic myocarditis from the scarred non-inflammatory myocardium, i.e. healed myocarditis.[166] Indeed, LGE and strain do not clearly differentiate between chronic and healed myocarditis,[167,168] whereas ^{18}F-FDG uptake decreases in the latter,[166] a feature that could help monitor treatment response to immunosuppressive therapy.[169] Given their complementary diagnostic values, studies have evaluated the value of hybrid ^{18}F-FDG PET/CMR in myocardial inflammatory diseases,[170,171] showing an incremental detection of cases with hybrid PET/CMR over single modalities alone.[172]

Early signs of cardiac dysfunction

Numerous efforts aim at detecting early-stage cardiac impairment, i.e. when anticancer treatment is still modifiable or cardioprotective measures can be introduced[8] (*Figure 6*).

Cardiac diastolic function

Diastolic dysfunction is a potential early marker of LV dysfunction,[173–175] which MUGA can assess. MUGA-derived diastolic function parameters include the peak filling rate, time-to-peak filling rate, and first third filling fraction[57,176–178] that deteriorate before treatment-induced systolic dysfunction.[177,179] However, the inter-

and intra-observer reproducibility of ERNA-based diastolic function is moderate,[57] questioning its utility in the early detection of CTRCD. CZT-based MUGA is promising, providing a highly reproducible assessment of diastolic function in cancer patients.[180] Still, MUGA is not routinely used to assess diastolic function, which can easily be obtained from echocardiography.[78] However, echocardiography is strongly operator-dependent, hampering its interest in surveillance.[74] CMR can also assess diastolic function based on LV mass and hypertrophy, LA size and function, mitral inflow and pulmonary venous velocity profiles, as well as myocardial deformation imaging with strain. Additionally, T1 mapping and ECV can be used.[181] CMR presents the advantage over echocardiography of highly reproducible and accurate volume measurements without geometrical or flat profile assumptions.[181] CMR's downsides are its restricted availability and the length of sequence acquisitions and image post-processing, limiting its routine use.[181]

Cardiac sympathetic innervation

Iodine-123 metaiodobenzylguanidine (^{123}I-MIBG) reflects the uptake, storage, and release of norepinephrine in the synaptic cleft,[182] hence allowing cardiac sympathetic innervation imaging.[183] The main parameter is the heart-to-mediastinum ratio (HMR),[184,185] i.e. the ratio between cardiac ^{123}I-MIBG uptake and a mediastinal reference region of interest. A diminished HMR indicates cardiac sympathetic denervation, either functional (downregulation of post-synaptic β-adrenergic receptors) or due to direct damage (for example, after toxic treatments[186]).

In patients receiving anthracycline, the HMR drops before LVEF,[187,188] highlighting ^{123}I-MIBG's potential role in early damage detection. Additionally, serial follow-up with cardiac ^{123}I-MIBG scintigraphy shows a slight dose-dependent sympathetic impairment following anthracycline administration,[187,189,190] suggesting a role in damage quantification.

PET radiotracers can also assess cardiac sympathetic activity,[191,192] notably 6-fluoro-^{18}F-L-dihydroxyphenylalanine (^{18}F-DOPA), an analogue of L-dihydroxyphenylalanine (L-DOPA) routinely used to investigate neuroendocrine tumours.[193] Another norepinephrine analogue is carbon-11-radiolabelled hydroxyephedrine (^{11}C-HED),[194] in which the need for on-site production limits clinical use. To date, however, no study has specifically studied these radiotracers to diagnose CTRCD.

Myocardial metabolism

Cardiac metabolism is a balance between various fuels, depending on the substrate's bloodstream availability, dietary conditions, and underlying myocardial conditions.[195] Under physiologic conditions, free fatty acids (FFAs) and glucose represent the primary cardiac energy sources.[196] Myocardial glucose consumption can be imaged with ^{18}F-FDG and FFA uptake with beta-methyl-iodine-123 phenylpentadecanoic acid (BMIPP).[197] In the fasting phase, FFAs are abundantly available to the heart,[196] rendering BMIPP more advantageous for assessing cardiac metabolism than ^{18}F-FDG.[198] Nonetheless, BMIPP is only routinely used in Japan,[199] and one study reported BMIPP uptake reduction in patients receiving taxanes.[200] Conversely, ^{18}F-FDG PET is largely available and part of the routine oncological assessment. In patients treated with doxorubicin, an increased LV ^{18}F-FDG uptake from baseline to end-of-treatment PET is associated with a subsequent LVEF drop[85] and MACE.[201] Moreover, increased RV ^{18}F-FDG uptake predicts a higher cardiotoxicity risk.[202] Similarly, in chest radiotherapy patients, focal cardiac ^{18}F-FDG uptake is associated with myocardial damage,[203–205] a study pointing towards a relation between the radiotherapy dose and the intensity of ^{18}F-FDG uptake.[206] Focal ^{18}F-FDG cardiac uptake in cancer patients correlates highly with perfusion abnormalities on SPECT MPI,[207] giving potential mechanistic insights for the subsequent cardiotoxicity. Still, a significant drawback of ^{18}F-FDG PET is the high variability of cardiac uptake with diet and insulinaemia,[208] which could be reduced by prolonged fasting.[209] Additionally, ^{18}F-FDG myocardial uptake increases in the ischaemic myocardium, which, although limiting the specificity of ^{18}F-FDG patterns, could identify ischaemia onset.[210]

Alternatively, carbon-11 (^{11}C) radiotracers can be used to image myocardial metabolism. ^{11}C-acetate is taken up by cardiomyocytes and converted to acetyl-CoA, a substrate for energy production via the tricarboxylic acid cycle.[211] The rate of ^{11}C-acetate uptake is a marker of myocardial oxidative metabolism.[212] In a pre-clinical model of mice undergoing treatment by tyrosine kinase inhibitors, the myocardium showed a decrease in ^{11}C-acetate uptake concomitantly to an increase in ^{18}F-FDG uptake.[213] The short half-life of ^{11}C (~20 min), although interesting from a radiation exposure perspective, is the main factor limiting its routine use, as ^{11}C requires an on-site cyclotron.[211]

Mitochondrial metabolism

The bottleneck of all cellular energy pathways is the mitochondrial production of ATP. Several chemotherapies affect ATP production and lead to cell death, generally by increasing reactive oxygen species (ROS) production.[198] A PET radiotracer targeting ROS has recently been developed, named ^{18}F-6-(4-((1-(2-fluoroethyl)-1H-1,2,3-triazol-4-yl)methoxy)phenyl)-5-methyl-5,6-dihydrophenanthridine-3,8-diamine (^{18}F-DHMT). In a pre-clinical rodent model of anthracycline-induced cardiotoxicity, ^{18}F-DHMT evidenced an increased myocardial ROS production before any LV drop.[214] Another ROS-targeting radiotracer is ^{18}F-3-(3-fluoropropyl)-2-phenyl-2,3-dihydrobenzo[d]thiazole (^{18}F-FPBT), in which myocardial uptake is also increased in rats receiving anthracycline.[215] Deregulation of cardiomyocyte homeostasis by chemotherapy can manifest as mitochondrial membrane dysfunction, which can be explored with ^{18}F(4-fluorophenyl)triphenylphosphonium (^{18}F-FTPP+). In a swine model receiving intracoronary infusions of anthracycline, ^{18}F-FTPP+ showed a partial mitochondrial depolarization in myocardial areas distal to the infused vessel.[216] Recently, a radiotracer targeting TSPO, a translocator protein expressed in mitochondrial-activated microglia, has been validated in a model of myocardial infarction.[217] This pre-clinical study showed that an early myocardial uptake of ^{18}F-radiolabelled TSPO on PET predicted the subsequent LVEF reduction.

Cell death

A hallmark apoptosis feature is the exposition of phosphatidylserine at the cellular surface.[218] Technetium-99m (^{99m}Tc)-radiolabelled annexin V is a phosphatidylserine ligand that detects apoptotic cardiomyocytes.[219] In rats receiving doxorubicin, ^{99m}Tc-radiolabelled annexin V evidenced drug-induced toxicity in a dose-dependent manner before any functional impairment on echography.[220] Recently, PET apoptosis radiotracers have also been developed.[221] In a mouse model of experimentally induced anthracycline cardiotoxicity, ^{18}F-CP18, a substrate of the caspase 3 enzyme present in apoptotic cells,[222] evidenced apoptosis before any LVEF drop.[223] Another target is myosin, externalized by necrotic cells after membrane rupture. Preliminary clinical studies showed that increased myocardial uptake of an indium-111 (^{111}In)-radiolabelled antimyosin antibody preceded LVEF modifications in patients receiving anthracycline.[189,224,225]

Myocardial fibrosis

The cardiomyocyte loss induced by anticancer treatments is accompanied by myocardial fibroblast activation, leading to fibrotic ventricular remodelling, a condition of increased risk for heart failure.[226] Although echocardiography and CMR can detect cardiac fibrosis,

even at an early stage with mapping techniques,[227,228] fibrosis still indicates myocardial damage. Therefore, detecting the onset of fibrotic replacement could help initiate cardiac treatments at an early and reversible stage.[227] Fibroblast activation protein (FAP) is a transmembrane protease with enhanced expression in activated fibroblasts.[229] Recently, pre-clinical findings evidenced intense ^{68}Ga-FAPI myocardial uptake in areas of activated fibroblasts, conversely to no uptake in areas of advanced fibrosis.[230–232] Similar incidental cases of ^{68}Ga-FAPI cardiac uptake have been reported in cancer patients, unveiling myocardial ischaemia.[233] This suggests that ^{68}Ga-FAPI PET, likely to be used for cancer staging, could help simultaneously detect early stages of myocardial fibrosis. Moreover, ^{68}Ga-FAPI myocardial uptake could pre-date any LVEF decrease, suggesting a potential role in cardiotoxicity prediction.[234] Similarly, an ^{18}F-radiolabelled FAPI tracer (^{18}F-AlF-NOTA-FAPI-04) detects radiation-induced myocardial ischaemia before LVEF decreases, comforting the potential role of FAPI radiotracers for the early identification of cardiac damage.[235]

Future directions

One next step is to stratify the cardiotoxicity risk before treatment initiation. Predictive scores based on CVRFs and biological markers[94,236,237] could be augmented by non-invasive imaging. For example, myocardial ^{18}F-FDG uptake obtained from routine staging ^{18}F-FDG PET can help stratify the cardiovascular risk with no additional cost or radiation burden.[207] Cardiovascular risk stratification could also benefit from hybrid PET/CMR by combining CMR mapping techniques with the prognostic value of myocardial ^{18}F-FDG uptake to predict the MACE risk.[238,239]

Artificial intelligence (AI) is a potential game changer in cardio-oncology.[240,241] In 2619 cancer-free patients explored with SPECT MPI, a machine learning analysis combined with clinical data outperformed human analysis for MACE prediction.[242] Moreover, the higher reproducibility of machine learning could improve diagnostic confidence in uncertain myocarditis patterns, such as patchy ^{18}F-FDG myocardial uptake. AI also improves the characterization of several types of malignant masses,[243–245] which might benefit cardiac tumour characterization.

In the era of precision medicine, where similar phenotypes arise from different genomic, metabolomic, and proteomic profiles, it will be crucial to tailoring the diagnosis to the tumour's '-omic signature'.[246] As a metabolic tool targeting specific pathophysiological pathways, nuclear imaging will most certainly play a central role in precision cardio-oncology.[246] In addition to mapping cardiotoxicity, these probes might play a theranostic role, as with SSTR radiotracers, which help select patients in whom peptide receptor radionuclide therapy is indicated.[247] An unsuccessful attempt in this sense has been made with ^{111}In-labelled trastuzumab scintigraphy to predict cardiotoxicity from trastuzumab.[248] Yet, the theranostic field is still in its infancy, and the wideness of metabolic targets assessable with nuclear radiotracers renders this goal within reach.

Conclusion

The progress in anticancer treatment is progressively turning cancer into a chronic condition. Consequently, the new challenge in this population is slowly shifting towards tackling other mortality causes, particularly CVD. Nuclear imaging allows for diagnosing various cardiac complications of anticancer therapies, even at an early stage, is useful for disease monitoring, and is a promising tool for the risk stratification of patients receiving cardiotoxic treatments. In addition, nuclear imaging has the unique ability to target specific metabolic links in the cardiotoxicity cascade for either diagnosis or treatment. Leveraging radiotracers already used routinely in patients with cancer, such as ^{18}F-FDG and MPI tracers, could benefit this population with no additional cost or radiation exposure. Consequently, in the expanding field of cardio-oncology, nuclear medicine remains a central player that will most certainly remain at the forefront of the diagnostic armamentarium alongside cross-sectional imaging.

Acknowledgements

The graphical abstract, as well as *Figures 1*, *2*, *3*, *5*, and *6*, were created on (or using elements/templates from) BioRender.com.

Funding

None declared.

Conflict of interest: All authors have the following to disclose. The University Hospital of Zurich holds a research contract with GE Healthcare. C.G. has received research grants from the Novartis Foundation, Switzerland. A.M. has provided a consulting, advisory, or speaker role for Amgen, Astellas, Boehringer Ingelheim, Bristol Myers Squibb, Celgene, Gerresheimer, GSK, Janssen, Merck, MSD, Novartis, Roche, Sanofi, Servier, Takeda, and Vifor; has received research funding from Bayer, Sanofi, Gerresheimer (personal), and Merck & Cie (institutional); has intellectual property interests relating to Merck & Cie (not related to this report); has been paid to provide expert testimony for Sanofi; and has reported travel/accommodation expenses paid for by Amgen, Astellas, Boehringer Ingelheim, Janssen, Merck, Roche, Sanofi, and Servier.

Data availability

No new data were generated or analysed in support of this research.

References

1. (WHO) WHO. WHO. The top 10 causes of death. 2020 2020 [cited 2022 2022 April 14]. Available from: https://www.who.int/news-room/fact-sheets/detail/the-top-10-causes-of-death.
2. Masoudkabir F, Sarrafzadegan N, Gotay C, Ignaszewski A, Krahn AD, Davis MK *et al.* Cardiovascular disease and cancer: evidence for shared disease pathways and pharmacologic prevention. *Atherosclerosis* 2017;**263**:343–51.
3. Handy CE, Quispe R, Pinto X, Blaha MJ, Blumenthal RS, Michos ED *et al.* Synergistic opportunities in the interplay between cancer screening and cardiovascular disease risk assessment: together we are stronger. *Circulation* 2018;**138**:727–34.
4. Johnson CB, Davis MK, Law A, Sulpher J. Shared risk factors for cardiovascular disease and cancer: implications for preventive health and clinical care in oncology patients. *Can J Cardiol* 2016;**32**:900–7.
5. Zhang X, Pawlikowski M, Olivo-Marston S, Williams KP, Bower JK, Felix AS. Ten-year cardiovascular risk among cancer survivors: the National Health and Nutrition Examination Survey. *PloS One* 2021;**16**:e0247919.
6. Lau ES, Paniagua SM, Liu E, Jovani M, Li SX, Takvorian K *et al.* Cardiovascular risk factors are associated with future cancer. *JACC CardioOncol* 2021;**3**:48–58.
7. van 't Klooster CC, Ridker PM, Cook NR, Aerts J, Westerink J, Asselbergs FW *et al.* Prediction of lifetime and 10-year risk of cancer in individual patients with established cardiovascular disease. *JACC CardioOncol* 2020;**2**:400–10.
8. Zamorano JL, Lancellotti P, Rodriguez Muñoz D, Aboyans V, Asteggiano R, Galderisi M *et al.* 2016 ESC Position Paper on cancer treatments and cardiovascular toxicity developed under the auspices of the ESC Committee for Practice Guidelines: the Task Force for cancer treatments and cardiovascular toxicity of the European Society of Cardiology (ESC). *Eur J Heart Fail* 2017;**19**:9–42.
9. Atkins KM, Rawal B, Chaunzwa TL, Lamba N, Bitterman DS, Williams CL *et al.* Cardiac radiation dose, cardiac disease, and mortality in patients with lung cancer. *J Am Coll Cardiol* 2019;**73**:2976–87.
10. Sturgeon KM, Deng L, Bluethmann SM, Zhou S, Trifiletti DM, Jiang C *et al.* A population-based study of cardiovascular disease mortality risk in US cancer patients. *Eur Heart J* 2019;**40**:3889–97.
11. Lyon AR, López-Fernández T, Couch LS, Asteggiano R, Aznar MC, Bergler-Klein J *et al.* 2022 ESC Guidelines on cardio-oncology developed in collaboration with the European Hematology Association (EHA), the European Society for Therapeutic Radiology and Oncology (ESTRO) and the International Cardio-Oncology Society (IC-OS). *Eur Heart J* 2022;**43**:4229–361.
12. Anker MS, Hadzibegovic S, Lena A, Belenkov Y, Bergler-Klein J, de Boer RA *et al.* Recent advances in cardio-oncology: a report from the 'Heart Failure Association 2019 and World Congress on Acute Heart Failure 2019'. *ESC Heart Fail* 2019;**6**:1140–8.

13. Curigliano G, Lenihan D, Fradley M, Ganatra S, Barac A, Blaes A *et al.* Management of cardiac disease in cancer patients throughout oncological treatment: ESMO consensus recommendations. *Ann Oncol* 2020;**31**:171–90.
14. Čelutkienė J, Pudil R, López-Fernández T, Grapsa J, Nihoyannopoulos P, Bergler-Klein J *et al.* Role of cardiovascular imaging in cancer patients receiving cardiotoxic therapies: a position statement on behalf of the Heart Failure Association (HFA), the European Association of Cardiovascular Imaging (EACVI) and the Cardio-Oncology Council of the European Society of Cardiology (ESC). *Eur J Heart Fail* 2020;**22**:1504–24.
15. Mikail N, Pisani A, El Hatimi S, Hentic O, Lebtahi R, Poitier B *et al.* Early diagnosis and treatment of myocardial neuroendocrine tumor metastasis: the cornerstone role of multimodality imaging. *Circ Cardiovasc Imaging* 2021;**14**:e011857.
16. Mikail N, Males L, Hyafil F, Benali K, Deschamps L, Brochet E *et al.* Diagnosis and staging of cardiac masses: additional value of CMR with (18)F-FDG-PET compared to CMR with CECT. *Eur J Nucl Med Mol Imaging* 2022;**49**:2232–41.
17. de Boer RA, Aboumsallem JP, Bracun V, Leedy D, Cheng R, Patel S *et al.* A new classification of cardio-oncology syndromes. *Cardiooncology* 2021;**7**:24.
18. Tocchetti CG, Ameri P, de Boer RA, D'Alessandra Y, Russo M, Sorriento D *et al.* Cardiac dysfunction in cancer patients: beyond direct cardiomyocyte damage of anticancer drugs: novel cardio-oncology insights from the joint 2019 meeting of the ESC Working Groups of Myocardial Function and Cellular Biology of the Heart. *Cardiovasc Res* 2020;**116**:1820–34.
19. Visseren FLJ, Mach F, Smulders YM, Carballo D, Koskinas KC, Bäck M *et al.* 2021 ESC Guidelines on cardiovascular disease prevention in clinical practice. *Eur Heart J* 2021; **42**:3227–337.
20. Meijers WC, de Boer RA. Common risk factors for heart failure and cancer. *Cardiovasc Res* 2019;**115**:844–53.
21. Giovannucci E, Harlan DM, Archer MC, Bergenstal RM, Gapstur SM, Habel LA *et al.* Diabetes and cancer: a consensus report. *Diabetes Care* 2010;**33**:1674–85.
22. Stocks T, Van Hemelrijck M, Manjer J, Bjørge T, Ulmer H, Hallmans G *et al.* Blood pressure and risk of cancer incidence and mortality in the Metabolic Syndrome and Cancer Project. *Hypertension* 2012;**59**:802–10.
23. Godtfredsen NS, Prescott E, Osler M. Effect of smoking reduction on lung cancer risk. *JAMA* 2005;**294**:1505–10.
24. Freedman ND, Silverman DT, Hollenbeck AR, Schatzkin A, Abnet CC. Association between smoking and risk of bladder cancer among men and women. *JAMA* 2011;**306**: 737–45.
25. Lauby-Secretan B, Scoccianti C, Loomis D, Grosse Y, Bianchini F, Straif K. Body fatness and cancer—viewpoint of the IARC Working Group. *N Engl J Med* 2016;**375**:794–8.
26. Kim Y, Seidman JG, Seidman CE. Genetics of cancer therapy-associated cardiotoxicity. *J Mol Cell Cardiol* 2022;**167**:85–91.
27. Genovese G, Kähler AK, Handsaker RE, Lindberg J, Rose SA, Bakhoum SF *et al.* Clonal hematopoiesis and blood-cancer risk inferred from blood DNA sequence. *N Engl J Med* 2014;**371**:2477–87.
28. Fuster JJ, Walsh K. Somatic mutations and clonal hematopoiesis: unexpected potential new drivers of age-related cardiovascular disease. *Circ Res* 2018;**122**:523–32.
29. Ewer MS, Lippman SM. Type II chemotherapy-related cardiac dysfunction: time to recognize a new entity. *J Clin Oncol* 2005;**23**:2900–2.
30. Ewer MS, Vooletich MT, Durand JB, Woods ML, Davis JR, Valero V *et al.* Reversibility of trastuzumab-related cardiotoxicity: new insights based on clinical course and response to medical treatment. *J Clin Oncol* 2005;**23**:7820–6.
31. Leiva O, AbdelHameid D, Connors JM, Cannon CP, Bhatt DL. Common pathophysiology in cancer, atrial fibrillation, atherosclerosis, and thrombosis: JACC: CardioOncology State-of-the-Art Review. *JACC CardioOncol* 2021;**3**:619–34.
32. Zaborowska-Szmit M, Krzakowski M, Kowalski DM, Szmit S. Cardiovascular complications of systemic therapy in non-small-cell lung cancer. *J Clinical medicine* 2020;**9**:1268.
33. Koutroumpakis E, Deswal A, Yusuf SW, Abe JI, Nead KT, Potter AS *et al.* Radiation-induced cardiovascular disease: mechanisms, prevention, and treatment. *Curr Oncol Rep* 2022;**24**:543–53.
34. Park BC, Stone CA Jr, Dewan AK, Johnson DB. Hypersensitivity reactions and immune-related adverse events to immune checkpoint inhibitors: approaches, mechanisms, and models. *Immunol Allergy Clin North Am* 2022;**42**:285–305.
35. Dehghani L, Mikail N, Kramkimel N, Soyer P, Lebtahi R, Mallone R *et al.* Autoimmune pancreatitis after nivolumab anti-programmed death receptor-1 treatment. *Eur J Cancer* 2018;**104**:243–6.
36. Lyon AR, Yousaf N, Battisti NML, Moslehi J, Larkin J. Immune checkpoint inhibitors and cardiovascular toxicity. *Lancet Oncol* 2018;**19**:e447–e58.
37. Čelutkienė J, Plymen CM, Flachskampf FA, de Boer RA, Grapsa J, Manka R *et al.* Innovative imaging methods in heart failure: a shifting paradigm in cardiac assessment. Position statement on behalf of the Heart Failure Association of the European Society of Cardiology. *Eur J Heart Fail* 2018;**20**:1615–33.
38. Cardinale D, Colombo A, Bacchiani G, Tedeschi I, Meroni CA, Veglia F *et al.* Early detection of anthracycline cardiotoxicity and improvement with heart failure therapy. *Circulation* 2015;**131**:1981–8.
39. Nagata Y, Takeuchi M, Mizukoshi K, Wu VC, Lin FC, Negishi K *et al.* Intervendor variability of two-dimensional strain using vendor-specific and vendor-independent software. *J Am Soc Echocardiogr* 2015;**28**:630–41.
40. Alexander J, Dainiak N, Berger HJ, Goldman L, Johnstone D, Reduto L *et al.* Serial assessment of doxorubicin cardiotoxicity with quantitative radionuclide angiocardiography. *N Engl J Med* 1979;**300**:278–83.
41. Choi BW, Berger HJ, Schwartz PE, Alexander J, Wackers FJ, Gottschalk A *et al.* Serial radionuclide assessment of doxorubicin cardiotoxicity in cancer patients with abnormal baseline resting left ventricular performance. *Am Heart J* 1983;**106**:638–43.
42. Jafari F, Safaei AM, Hosseini L, Asadian S, Kamangar TM, Zadehbagheri F *et al.* The role of cardiac magnetic resonance imaging in the detection and monitoring of cardiotoxicity in patients with breast cancer after treatment: a comprehensive review. *Heart Fail Rev* 2021;**26**:679–97.
43. Cadour F, Thuny F, Sourdon J. New insights in early detection of anticancer drug-related cardiotoxicity using perfusion and metabolic imaging. *Front Cardiovasc Med* 2022;**9**:813883.
44. Soufer A, Liu C, Henry ML, Baldassarre LA. Nuclear cardiology in the context of multimodality imaging to detect cardiac toxicity from cancer therapeutics: established and emerging methods. *J Nucl Cardiol* 2020;**27**:1210–24.
45. Polomski ES, Antoni ML, Jukema JW, Kroep JR, Dibbets-Schneider P, Sattler MGA *et al.* Nuclear medicine imaging methods of radiation-induced cardiotoxicity. *Semin Nucl Med* 2022;**52**:597–610.
46. Plana JC, Galderisi M, Barac A, Ewer MS, Ky B, Scherrer-Crosbie M *et al.* Expert consensus for multimodality imaging evaluation of adult patients during and after cancer therapy: a report from the American Society of Echocardiography and the European Association of Cardiovascular Imaging. *Eur Heart J Cardiovasc Imaging* 2014;**15**:1063–93.
47. Dhir V, Yan AT, Nisenbaum R, Sloninko J, Connelly KA, Barfett J *et al.* Assessment of left ventricular function by CMR versus MUGA scans in breast cancer patients receiving trastuzumab: a prospective observational study. *Int J Cardiovasc Imaging* 2019;**35**: 2085–93.
48. Printezi MI, Yousif LIE, Kamphuis JAM, van Laake LW, Cramer MJ, Hobbelink MGG *et al.* LVEF by multigated acquisition scan compared to other imaging modalities in cardio-oncology: a systematic review. *Curr Heart Fail Rep* 2022;**19**:136–45.
49. Odak M, Kayani WT. MUGA Scan. StatPearls. Treasure Island (FL): StatPearls Publishing Copyright © 2022, StatPearls Publishing LLC; 2022.
50. Hesse B, Lindhardt TB, Acampa W, Anagnostopoulos C, Ballinger J, Bax JJ *et al.* EANM/ESC Guidelines for radionuclide imaging of cardiac function. *Eur J Nucl Med Mol Imaging* 2008;**35**:851–85.
51. Paul AK, Nabi HA. Gated myocardial perfusion SPECT: basic principles, technical aspects, and clinical applications. *J Nucl Med Technol* 2004;**32**:179–87; quiz 88–9.
52. Zhao J, Peng M, Xu L. Equilibrium radionuclide angiocardiography for the evaluation of right ventricular ejection fraction in patients with cardiac disorders. *Int J Clin Exp Med* 2015;**8**:18144–50.
53. Chin BB, Bloomgarden DC, Xia W, Kim HJ, Fayad ZA, Ferrari VA *et al.* Right and left ventricular volume and ejection fraction by tomographic gated blood-pool scintigraphy. *J Nucl Med* 1997;**38**:942–8.
54. Xie BQ, Tian YQ, Zhang J, Zhao SH, Yang MF, Guo F *et al.* Evaluation of left and right ventricular ejection fraction and volumes from gated blood-pool SPECT in patients with dilated cardiomyopathy: comparison with cardiac MRI. *J Nucl Med* 2012;**53**: 584–91.
55. Dercle L, Ouali M, Pascal P, Giraudmaillet T, Chisin R, Lairez O *et al.* Gated blood pool SPECT: the estimation of right ventricular volume and function is algorithm dependent in a clinical setting. *J Nucl Cardiol* 2015;**22**:483–92.
56. Dercle L, Giraudmaillet T, Pascal P, Lairez O, Chisin R, Marachet MA *et al.* Is TOMPOOL (gated blood-pool SPECT processing software) accurate to diagnose right and left ventricular dysfunction in a clinical setting? *J Nucl Cardiol* 2014;**21**: 1011–22.
57. Sachpekidis C, Sachpekidis V, Kopp-Schneider A, Arsos G, Moralidis E. Equilibrium radionuclide angiography: intra- and inter-observer repeatability and reproducibility in the assessment of cardiac systolic and diastolic function. *J Nucl Cardiol* 2021;**28**: 1304–14.
58. Doherty JU, Kort S, Mehran R, Schoenhagen P, Soman P. ACC/AATS/AHA/ASE/ASNC/HRS/SCAI/SCCT/SCMR/STS 2019 appropriate use criteria for multimodality imaging in the assessment of cardiac structure and function in nonvalvular heart disease: a report of the American College of Cardiology Appropriate Use Criteria Task Force, American Association for Thoracic Surgery, American Heart Association, American Society of Echocardiography, American Society of Nuclear Cardiology, Heart Rhythm Society, Society for Cardiovascular Angiography and Interventions, Society of Cardiovascular Computed Tomography, Society for Cardiovascular Magnetic Resonance, and the Society of Thoracic Surgeons. *J Nucl Cardiol* 2019;**26**:1392–413.
59. Schwartz RG, McKenzie WB, Alexander J, Sager P, D'Souza A, Manatunga A *et al.* Congestive heart failure and left ventricular dysfunction complicating doxorubicin

therapy. Seven-year experience using serial radionuclide angiocardiography. *Am J Med* 1987;**82**:1109–18.
60. Liu YH, Fazzone-Chettiar R, Sandoval V, Tsatkin V, Miller EJ, Sinusas AJ. New approach for quantification of left ventricular function from low-dose gated bloodpool SPECT: validation and comparison with conventional methods in patients. *J Nucl Cardiol* 2021; **28**:939–50.
61. Groch MW, DePuey EG, Belzberg AC, Erwin WD, Kamran M, Barnett CA *et al.* Planar imaging versus gated blood-pool SPECT for the assessment of ventricular performance: a multicenter study. *J Nucl Med* 2001;**42**:1773–9.
62. Huang H, Nijjar PS, Misialek JR, Blaes A, Derrico NP, Kazmirczak F *et al.* Accuracy of left ventricular ejection fraction by contemporary multiple gated acquisition scanning in patients with cancer: comparison with cardiovascular magnetic resonance. *J Cardiovasc Magn Reson* 2017;**19**:34.
63. Luu JM, Gebhard C, Ramasundarahettige C, Desai D, Schulze K, Marcotte F *et al.* Normal sex and age-specific parameters in a multi-ethnic population: a cardiovascular magnetic resonance study of the Canadian Alliance for Healthy Hearts and Minds cohort. *J Cardiovasc Magn Reson* 2022;**24**:2.
64. Mikail N, Rossi A, Bengs S, Haider A, Stähli BE, Portmann A *et al.* Imaging of heart disease in women: review and case presentation. *Eur J Nucl Med Mol Imaging* 2022;**50**: 130–59.
65. Farrell MB, Galt JR, Georgoulias P, Malhotra S, Pagnanelli R, Rischpler C *et al.* SNMMI procedure standard/EANM guideline for gated equilibrium radionuclide angiography. *J Nucl Med Technol* 2020;**48**:126–35.
66. Carpeggiani C, Rossi G, Landi P, Michelassi C, Brambilla M, Cortigiani L *et al.* Long-term outcome and medical radiation exposure in patients hospitalized for cardiovascular disease. *Int J Cardiol* 2015;**195**:30–6.
67. Laskey WK, Feinendegen LE, Neumann RD, Dilsizian V. Low-level ionizing radiation from noninvasive cardiac imaging: can we extrapolate estimated risks from epidemiologic data to the clinical setting? *JACC Cardiovasc Imaging* 2010;**3**:517–24.
68. Doukky R, Frogge N, Appis A, Hayes K, Khoudary G, Fogg L *et al.* Impact of appropriate use on the estimated radiation risk to men and women undergoing radionuclide myocardial perfusion imaging. *J Nucl Med* 2016;**57**:1251–7.
69. Tissot H, Roch V, Morel O, Veran N, Perrin M, Claudin M *et al.* Left ventricular ejection fraction determined with the simulation of a very low-dose CZT-SPECT protocol and an additional count-calibration on planar radionuclide angiographic data. *J Nucl Cardiol* 2019;**26**:1539–49.
70. Claudin M, Imbert L, Djaballah W, Veran N, Poussier S, Roch V *et al.* Routine evaluation of left ventricular function using CZT-SPECT, with low injected activities and limited recording times. *J Nucl Cardiol* 2018;**25**:249–56.
71. Chen YC, Ko CL, Yen RF, Lo MF, Huang YH, Hsu PY *et al.* Comparison of biventricular ejection fractions using cadmium-zinc-telluride SPECT and planar equilibrium radionuclide angiography. *J Nucl Cardiol* 2016;**23**:348–61.
72. Apert A, Canu M, Jankowski A, Riou L, Broisat A, Charlon C *et al.* Comparison of cadmium zinc telluride ECG-gated SPECT equilibrium radionuclide angiocardiography to magnetic resonance imaging to measure right ventricular volumes and ejection fraction in patients with cardiomyopathy. *J Nucl Cardiol* 2022;**29**:1647–56.
73. Bouallègue FB, Maïmoun L, Kucharczak F, Le Fur P, Vauchot F, Hay B *et al.* Left ventricle function assessment using gated first-pass (18)F-FDG PET: validation against equilibrium radionuclide angiography. *J Nucl Cardiol* 2021;**28**:594–603.
74. Lang RM, Badano LP, Mor-Avi V, Afilalo J, Armstrong A, Ernande L *et al.* Recommendations for cardiac chamber quantification by echocardiography in adults: an update from the American Society of Echocardiography and the European Association of Cardiovascular Imaging. *Eur Heart J Cardiovasc Imaging* 2015;**16**:233–70.
75. Plana JC, Thavendiranathan P, Bucciarelli-Ducci C, Lancellotti P. Multi-modality imaging in the assessment of cardiovascular toxicity in the cancer patient. *JACC Cardiovasc Imaging* 2018;**11**:1173–86.
76. Thavendiranathan P, Grant AD, Negishi T, Plana JC, Popović ZB, Marwick TH. Reproducibility of echocardiographic techniques for sequential assessment of left ventricular ejection fraction and volumes: application to patients undergoing cancer chemotherapy. *J Am Coll Cardiol* 2013;**61**:77–84.
77. Thavendiranathan P, Negishi T, Somerset E, Negishi K, Penicka M, Lemieux J *et al.* Strain-guided management of potentially cardiotoxic cancer therapy. *J Am Coll Cardiol* 2021;**77**:392–401.
78. Zamorano JL, Lancellotti P, Rodriguez Muñoz D, Aboyans V, Asteggiano R, Galderisi M *et al.* 2016 ESC Position Paper on cancer treatments and cardiovascular toxicity developed under the auspices of the ESC Committee for Practice Guidelines: the Task Force for cancer treatments and cardiovascular toxicity of the European Society of Cardiology (ESC). *Eur Heart J* 2016;**37**:2768–801.
79. Meléndez GC, Sukpraphrute B, D'Agostino RB, Jordan JH, Klepin HD, Ellis L *et al.* Frequency of left ventricular end-diastolic volume-mediated declines in ejection fraction in patients receiving potentially cardiotoxic cancer treatment. *Am J Cardiol* 2017; **119**:1637–42.
80. Ylänen K, Poutanen T, Savikurki-Heikkilä P, Rinta-Kiikka I, Eerola A, Vettenranta K. Cardiac magnetic resonance imaging in the evaluation of the late effects of anthracyclines among long-term survivors of childhood cancer. *J Am Coll Cardiol* 2013;**61**:1539–47.
81. O'Quinn R, Ferrari VA, Daly R, Hundley G, Baldassarre LA, Han Y *et al.* Cardiac magnetic resonance in cardio-oncology: advantages, importance of expediency, and considerations to navigate pre-authorization. *JACC CardioOncol* 2021;**3**:191–200.
82. Altaha MA, Nolan M, Marwick TH, Somerset E, Houbois C, Amir E *et al.* Can quantitative CMR tissue characterization adequately identify cardiotoxicity during chemotherapy? : impact of temporal and observer variability. *JACC Cardiovasc Imaging* 2020; **13**:951–62.
83. Pickett CA, Cheezum MK, Kassop D, Villines TC, Hulten EA. Accuracy of cardiac CT, radionucleotide and invasive ventriculography, two- and three-dimensional echocardiography, and SPECT for left and right ventricular ejection fraction compared with cardiac MRI: a meta-analysis. *Eur Heart J Cardiovasc Imaging* 2015;**16**:848–52.
84. Hoffmann R, Barletta G, von Bardeleben S, Vanoverschelde JL, Kasprzak J, Greis C *et al.* Analysis of left ventricular volumes and function: a multicenter comparison of cardiac magnetic resonance imaging, cine ventriculography, and unenhanced and contrast-enhanced two-dimensional and three-dimensional echocardiography. *J Am Soc Echocardiogr* 2014;**27**:292–301.
85. Sarocchi M, Bauckneht M, Arboscello E, Capitanio S, Marini C, Morbelli S *et al.* An increase in myocardial 18-fluorodeoxyglucose uptake is associated with left ventricular ejection fraction decline in Hodgkin lymphoma patients treated with anthracycline. *J Transl Med* 2018;**16**:295.
86. Li J, Zhao J, Lei Y, Chen Y, Cheng M, Wei X *et al.* Coronary atherosclerotic disease and cancer: risk factors and interrelation. *Front Cardiovasc Med* 2022;**9**:821267.
87. Aronson D, Brenner B. Arterial thrombosis and cancer. *Thromb Res* 2018;**164**:S23–S8.
88. van Nimwegen FA, Schaapveld M, Janus CP, Krol AD, Petersen EJ, Raemaekers JM *et al.* Cardiovascular disease after Hodgkin lymphoma treatment: 40-year disease risk. *JAMA Int Med* 2015;**175**:1007–17.
89. Pak S, Hawash AA, Linares J, Valencia D, Kilgore A, Valencia V *et al.* Myocardial damage on SPECT imaging among patients treated with radiotherapy for left-sided breast cancer: systematic review with meta-analysis and narrative synthesis. *J BUON* 2018;**23**: 910–8.
90. Mitchell JD, Cehic DA, Morgia M, Bergom C, Toohey J, Guerrero PA *et al.* Cardiovascular manifestations from therapeutic radiation: a multidisciplinary expert consensus statement from the International Cardio-Oncology Society. *JACC CardioOncol* 2021;**3**:360–80.
91. Desai MY, Windecker S, Lancellotti P, Bax JJ, Griffin BP, Cahlon O *et al.* Prevention, diagnosis, and management of radiation-associated cardiac disease: JACC Scientific Expert Panel. *J Am Coll Cardiol* 2019;**74**:905–27.
92. Saraste A, Barbato E, Capodanno D, Edvardsen T, Prescott E, Achenbach S *et al.* Imaging in ESC clinical guidelines: chronic coronary syndromes. *Eur Heart J Cardiovasc Imaging* 2019;**20**:1187–97.
93. Zhang P, Hu X, Yue J, Meng X, Han D, Sun X *et al.* Early detection of radiation-induced heart disease using (99m)Tc-MIBI SPECT gated myocardial perfusion imaging in patients with oesophageal cancer during radiotherapy. *Radiother Oncol* 2015;**115**:171–8.
94. Darby SC, Ewertz M, McGale P, Bennet AM, Blom-Goldman U, Brønnum D *et al.* Risk of ischemic heart disease in women after radiotherapy for breast cancer. *N Engl J Med* 2013;**368**:987–98.
95. Gyenes G, Fornander T, Carlens P, Glas U, Rutqvist LE. Detection of radiation-induced myocardial damage by technetium-99m sestamibi scintigraphy. *Eur J Nucl Med* 1997; **24**:286–92.
96. Seddon B, Cook A, Gothard L, Salmon E, Latus K, Underwood SR *et al.* Detection of defects in myocardial perfusion imaging in patients with early breast cancer treated with radiotherapy. *Radiother Oncol* 2002;**64**:53–63.
97. Bergom C, Bradley JA, Ng AK, Samson P, Robinson C, Lopez-Mattei J *et al.* Past, present, and future of radiation-induced cardiotoxicity: refinements in targeting, surveillance, and risk stratification. *JACC CardioOncol* 2021;**3**:343–59.
98. Correa CR, Litt HI, Hwang WT, Ferrari VA, Solin LJ, Harris EE. Coronary artery findings after left-sided compared with right-sided radiation treatment for early-stage breast cancer. *J Clin Oncol* 2007;**25**:3031–7.
99. Kaidar-Person O, Zagar TM, Oldan JD, Matney J, Jones EL, Das S *et al.* Early cardiac perfusion defects after left-sided radiation therapy for breast cancer: is there a volume response? *Breast Cancer Res Treat* 2017;**164**:253–62.
100. Marks LB, Yu X, Prosnitz RG, Zhou SM, Hardenbergh PH, Blazing M *et al.* The incidence and functional consequences of RT-associated cardiac perfusion defects. *Int J Radiat Oncol Biol Phys* 2005;**63**:214–23.
101. Quintero-Martinez JA, Cordova-Madera SN, Villarraga HR. Radiation-induced heart disease. *J Clin Med* 2021;**11**:146.
102. Galán-Arriola C, Vílchez-Tschischke JP, Lobo M, López GJ, de Molina-Iracheta A, Pérez-Martínez C *et al.* Coronary microcirculation damage in anthracycline cardiotoxicity. *Cardiovasc Res* 2022;**118**:531–41.
103. Fabin N, Bergami M, Cenko E, Bugiardini R, Manfrini O. The role of vasospasm and microcirculatory dysfunction in fluoropyrimidine-induced ischemic heart disease. *J Clin Med* 2022;**11**:1244.

104. Schindler TH, Dilsizian V. Coronary microvascular dysfunction: clinical considerations and noninvasive diagnosis. *JACC Cardiovasc Imaging* 2020;**13**:140–55.
105. Gould KL, Johnson NP. Coronary physiology beyond coronary flow reserve in microvascular angina: JACC State-of-the-Art Review. *J Am Coll Cardiol* 2018;**72**:2642–62.
106. Groarke JD, Divakaran S, Nohria A, Killoran JH, Dorbala S, Dunne RM *et al.* Coronary vasomotor dysfunction in cancer survivors treated with thoracic irradiation. *J Nucl Cardiol* 2021;**28**:2976–87.
107. Żyromska A, Małkowski B, Wiśniewski T, Majewska K, Reszke J, Makarewicz R. (15) O-H(2)O PET/CT as a tool for the quantitative assessment of early post-radiotherapy changes of heart perfusion in breast carcinoma patients. *Br J Radiol* 2018;**91**:20170653.
108. Divakaran S, Caron JP, Zhou W, Hainer J, Bibbo CF, Skali H *et al.* Coronary vasomotor dysfunction portends worse outcomes in patients with breast cancer. *J Nucl Cardiol* 2022;**29**:3072–81.
109. Hecht HS, Cronin P, Blaha MJ, Budoff MJ, Kazerooni EA, Narula J *et al.* 2016 SCCT/STR guidelines for coronary artery calcium scoring of noncontrast noncardiac chest CT scans: a report of the Society of Cardiovascular Computed Tomography and Society of Thoracic Radiology. *J Cardiovasc Comput Tomogr* 2017;**11**:74–84.
110. Cainzos-Achirica M, Nasir K. Debates in cardiac CT: the force of data is with CAC—and it's rock solid. *J Cardiovasc Comput Tomogr* 2022;**16**:286–9.
111. Chang SM, Nabi F, Xu J, Peterson LE, Achari A, Pratt CM *et al.* The coronary artery calcium score and stress myocardial perfusion imaging provide independent and complementary prediction of cardiac risk. *J Am Coll Cardiol* 2009;**54**:1872–82.
112. Einstein AJ, Johnson LL, Bokhari S, Son J, Thompson RC, Bateman TM *et al.* Agreement of visual estimation of coronary artery calcium from low-dose CT attenuation correction scans in hybrid PET/CT and SPECT/CT with standard Agatston score. *J Am Coll Cardiol* 2010;**56**:1914–21.
113. Sharma V, Mughal L, Dimitropoulos G, Sheikh A, Griffin M, Moss A *et al.* The additive prognostic value of coronary calcium score (CCS) to single photon emission computed tomography myocardial perfusion imaging (SPECT-MPI)-real world data from a single center. *J Nucl Cardiol* 2021;**28**:2086–96.
114. McConachie P, McKay E, Crane A, Nguyen N, Quinn R, Butler SP. Accurate measurement of coronary artery calcium in cancer patients using the CT component of PET/CT scans. *Nucl Med Commun* 2022;**43**:159–65.
115. Pope A, Thomson L, Cantu S, Setia G, Torosyan N, Merz NB *et al.* Detection of subclinical atherosclerosis from PET-CT in patients with breast cancer. *J Cardiovasc Comput Tomogr* 2022;**16**:189–90.
116. de Amorim Fernandes F, Peix A, Giubbini R, Karthikeyan G, Massardo T, Patel C *et al.* Reproducibility of global LV function and dyssynchrony parameters derived from phase analysis of gated myocardial perfusion SPECT: a multicenter comparison with core laboratory setting. *J Nucl Cardiol* 2020;**29**:952–61.
117. Bouallègue F B, Mariano-Goulart D, Agostini D, Manrique A. Feasibility of biventricular volume and function assessment using first-pass gated (15)O-water PET. *EJNMMI Res* 2018;**8**:92.
118. Manrique A, Faraggi M, Véra P, Vilain D, Lebtahi R, Cribier A *et al.* 201Tl and 99mTc-MIBI gated SPECT in patients with large perfusion defects and left ventricular dysfunction: comparison with equilibrium radionuclide angiography. *J Nucl Med* 1999;**40**:805–9.
119. Jensen MM, Schmidt U, Huang C, Zerahn B. Gated tomographic radionuclide angiography using cadmium-zinc-telluride detector gamma camera; comparison to traditional gamma cameras. *J Nucl Cardiol* 2014;**21**:384–96.
120. Wu D, Zhang Z, Ma R, Guo F, Wang L, Fang W. Comparison of CZT SPECT and conventional SPECT for assessment of contractile function, mechanical synchrony and myocardial scar in patients with heart failure. *J Nucl Cardiol* 2019;**26**:443–52.
121. Pelletier-Galarneau M, Finnerty V, Tan S, Authier S, Gregoire J, Harel F. Assessment of left ventricular ejection fraction with cardiofocal collimators: comparison between IQ-SPECT, planar equilibrium radionuclide angiography, and cardiac magnetic resonance. *J Nucl Cardiol* 2019;**26**:1857–64.
122. Bailliez A, Lairez O, Merlin C, Piriou N, Legallois D, Blaire T *et al.* Left ventricular function assessment using 2 different cadmium-zinc-telluride cameras compared with a γ-camera with cardiofocal collimators: dynamic cardiac phantom study and clinical validation. *J Nucl Med* 2016;**57**:1370–5.
123. Whelton SP, Al Rifai M, Dardari Z, Shaw LJ, Al-Mallah MH, Matsushita K *et al.* Coronary artery calcium and the competing long-term risk of cardiovascular vs. cancer mortality: the CAC Consortium. *Eur Heart J Cardiovasc Imaging* 2019;**20**:389–95.
124. Gimelli A, Achenbach S, Buechel RR, Edvardsen T, Francone M, Gaemperli O *et al.* Strategies for radiation dose reduction in nuclear cardiology and cardiac computed tomography imaging: a report from the European Association of Cardiovascular Imaging (EACVI), the Cardiovascular Committee of European Association of Nuclear Medicine (EANM), and the European Society of Cardiovascular Radiology (ESCR). *Eur Heart J* 2018;**39**:286–96.
125. Plana JC, Galderisi M, Barac A, Ewer MS, Ky B, Scherrer-Crosbie M *et al.* Expert consensus for multimodality imaging evaluation of adult patients during and after cancer therapy: a report from the American Society of Echocardiography and the European Association of Cardiovascular Imaging. *J Am Soc Echocardiogr* 2014;**27**:911–39.
126. Cottin Y, L'Huillier I, Casasnovas O, Geoffroy C, Caillot D, Zeller M *et al.* Dobutamine stress echocardiography identifies anthracycline cardiotoxicity. *Eur J Echocardiogr* 2000;**1**:180–3.
127. Jarfelt M, Kujacic V, Holmgren D, Bjarnason R, Lannering B. Exercise echocardiography reveals subclinical cardiac dysfunction in young adult survivors of childhood acute lymphoblastic leukemia. *Pediatr Blood Cancer* 2007;**49**:835–40.
128. Civelli M, Cardinale D, Martinoni A, Lamantia G, Colombo N, Colombo A *et al.* Early reduction in left ventricular contractile reserve detected by dobutamine stress echo predicts high-dose chemotherapy-induced cardiac toxicity. *Int J Cardiol* 2006;**111**:120–6.
129. Rossi A, Wragg A, Klotz E, Pirro F, Moon JC, Nieman K *et al.* Dynamic computed tomography myocardial perfusion imaging: comparison of clinical analysis methods for the detection of vessel-specific ischemia. *Circ Cardiovasc Imaging* 2017;**10**:e005505.
130. de Knegt MC, Rossi A, Petersen SE, Wragg A, Khurram R, Westwood M *et al.* Stress myocardial perfusion with qualitative magnetic resonance and quantitative dynamic computed tomography: comparison of diagnostic performance and incremental value over coronary computed tomography angiography. *Eur Heart J Cardiovasc Imaging* 2020;**8**:jeaa270.
131. Kitagawa K, Nakamura S, Ota H, Ogawa R, Shizuka T, Kubo T *et al.* Diagnostic performance of dynamic myocardial perfusion imaging using dual-source computed tomography. *J Am Coll Cardiol* 2021;**78**:1937–49.
132. Nous FMA, Geisler T, Kruk MBP, Alkadhi H, Kitagawa K, Vliegenthart R *et al.* Dynamic myocardial perfusion CT for the detection of hemodynamically significant coronary artery disease. *JACC Cardiovasc Imaging* 2022;**15**:75–87.
133. Rahman H, Scannell CM, Demir OM, Ryan M, McConkey H, Ellis H *et al.* High-resolution cardiac magnetic resonance imaging techniques for the identification of coronary microvascular dysfunction. *JACC Cardiovasc Imaging* 2021;**14**:978–86.
134. Mathew RC, Bourque JM, Salerno M, Kramer CM. Cardiovascular imaging techniques to assess microvascular dysfunction. *JACC Cardiovasc Imaging* 2020;**13**:1577–90.
135. Taqueti VR, Di Carli MF. Coronary microvascular disease pathogenic mechanisms and therapeutic options: JACC State-of-the-Art Review. *J Am Coll Cardiol* 2018;**72**:2625–41.
136. Rasmussen LD, Winther S, Eftekhari A, Karim SR, Westra J, Isaksen C *et al.* Second-line myocardial perfusion imaging to detect obstructive stenosis: head-to-head comparison of CMR and PET. *JACC Cardiovasc Imaging* 2023;**16**:642–55.
137. Saiki H, Petersen IA, Scott CG, Bailey KR, Dunlay SM, Finley RR *et al.* Risk of heart failure with preserved ejection fraction in older women after contemporary radiotherapy for breast cancer. *Circulation* 2017;**135**:1388–96.
138. Banister HR, Hammond ST, Parr SK, Sutterfield SL, Turpin VG, Treinen S *et al.* Lower endothelium-dependent microvascular function in adult breast cancer patients receiving radiation therapy. *Cardiooncology* 2021;**7**:18.
139. Chen DS, Mellman I. Oncology meets immunology: the cancer-immunity cycle. *Immunity* 2013;**39**:1–10.
140. Stein-Merlob AF, Rothberg MV, Ribas A, Yang EH. Cardiotoxicities of novel cancer immunotherapies. *Heart* 2021;**107**:1694–703.
141. Malaty MM, Amarasekera AT, Li C, Scherrer-Crosbie M, Tan TC. Incidence of immune checkpoint inhibitor mediated cardiovascular toxicity: a systematic review and meta-analysis. *Eur J Clin Invest* 2022;**52**:e13831.
142. Ederhy S, Cautela J, Ancedy Y, Escudier M, Thuny F, Cohen A. Takotsubo-like syndrome in cancer patients treated with immune checkpoint inhibitors. *JACC Cardiovasc Imaging* 2018;**11**:1187–90.
143. Mahmood SS, Fradley MG, Cohen JV, Nohria A, Reynolds KL, Heinzerling LM *et al.* Myocarditis in patients treated with immune checkpoint inhibitors. *J Am Coll Cardiol* 2018;**71**:1755–64.
144. Ferreira VM, Schulz-Menger J, Holmvang G, Kramer CM, Carbone I, Sechtem U *et al.* Cardiovascular magnetic resonance in nonischemic myocardial inflammation: expert recommendations. *J Am Coll Cardiol* 2018;**72**:3158–76.
145. Ederhy S, Devos P, Pinna B, Funck-Brentano E, Abbar B, Fenioux C *et al.* (18) F-fluorodeoxyglucose positron emission tomography/computed tomography imaging for the diagnosis of immune checkpoint inhibitor-associated myocarditis. *Arch Cardiovasc Dis* 2022;**115**:114–6.
146. Ozawa K, Funabashi N, Daimon M, Takaoka H, Takano H, Uehara M *et al.* Determination of optimum periods between onset of suspected acute myocarditis and ^{18}F-fluorodeoxyglucose positron emission tomography in the diagnosis of inflammatory left ventricular myocardium. *Int J Cardiol* 2013;**169**:196–200.
147. Bonaca MP, Olenchock BA, Salem JE, Wiviott SD, Ederhy S, Cohen A *et al.* Myocarditis in the setting of cancer therapeutics: proposed case definitions for emerging clinical syndromes in cardio-oncology. *Circulation* 2019;**140**:80–91.
148. Nensa F, Kloth J, Tezgah E, Poeppel TD, Heusch P, Goebel J *et al.* Feasibility of FDG-PET in myocarditis: comparison to CMR using integrated PET/MRI. *J Nucl Cardiol* 2018;**25**:785–94.
149. Tarkin JM, Joshi FR, Evans NR, Chowdhury MM, Figg NL, Shah AV *et al.* Detection of atherosclerotic inflammation by (68)Ga-DOTATATE PET compared to [(18)F]FDG PET imaging. *J Am Coll Cardiol* 2017;**69**:1774–91.

150. Lee H, Schubert EK, Vidula MK, Pryma DA, Marchlinski FE, Goldberg LR *et al.* Potential clinical utility of (68)Ga-DOTATATE PET/CT for detection and response assessment in cardiac sarcoidosis. *J Nucl Cardiol* 2022;**30**:1075–87.
151. Boughdad S, Latifyan S, Fenwick C, Bouchaab H, Suffiotti M, Moslehi JJ *et al.* (68) Ga-DOTATOC PET/CT to detect immune checkpoint inhibitor-related myocarditis. *J Immunother Cancer* 2021;**9**:e003594.
152. Giesel FL, Kratochwil C, Lindner T, Marschalek MM, Loktev A, Lehnert W *et al.* (68) Ga-FAPI PET/CT: biodistribution and preliminary dosimetry estimate of 2 DOTA-containing FAP-targeting agents in patients with various cancers. *J Nucl Med* 2019;**60**:386–92.
153. Kratochwil C, Flechsig P, Lindner T, Abderrahim L, Altmann A, Mier W *et al.* (68) Ga-FAPI PET/CT: tracer uptake in 28 different kinds of cancer. *J Nucl Med* 2019;**60**: 801–5.
154. Finke D, Heckmann MB, Herpel E, Katus HA, Haberkorn U, Leuschner F *et al.* Early detection of checkpoint inhibitor-associated myocarditis using (68)Ga-FAPI PET/CT. *Front Cardiovasc Med* 2021;**8**:614997.
155. Vorster M. Gallium-68 labelled radiopharmaceuticals for imaging inflammatory disorders. *Semin Nucl Med* 2023;**53**:199–212.
156. Glasenapp A, Derlin K, Gutberlet M, Hess A, Ross TL, Wester HJ *et al.* Molecular imaging of inflammation and fibrosis in pressure overload heart failure. *Circ Res* 2021;**129**: 369–82.
157. Kircher M, Lapa C. Novel noninvasive nuclear medicine imaging techniques for cardiac inflammation. *Curr Cardiovasc Imaging Rep* 2017;**10**:6.
158. Kristensen LK, Fröhlich C, Christensen C, Melander MC, Poulsen TT, Galler GR *et al.* CD4(+) And CD8a(+) PET imaging predicts response to novel PD-1 checkpoint inhibitor: studies of Sym021 in syngeneic mouse cancer models. *Theranostics* 2019;**9**: 8221–38.
159. Maslov DV, Tawagi K, Kc M, Simenson V, Yuan H, Parent C *et al.* Timing of steroid initiation and response rates to immune checkpoint inhibitors in metastatic cancer. *J Immunother Cancer* 2021;**9**:e002261.
160. Ferreira VM, Schulz-Menger J, Holmvang G, Kramer CM, Carbone I, Sechtem U *et al.* Cardiovascular magnetic resonance in nonischemic myocardial inflammation: expert recommendations. *J Am Coll Cardiol* 2018;**72**:3158–76.
161. Friedrich MG, Sechtem U, Schulz-Menger J, Holmvang G, Alakija P, Cooper LT *et al.* Cardiovascular magnetic resonance in myocarditis: a JACC White Paper. *J Am Coll Cardiol* 2009;**53**:1475–87.
162. Quinaglia T, Gongora C, Awadalla M, Hassan MZO, Zafar A, Drobni ZD *et al.* Global circumferential and radial strain among patients with immune checkpoint inhibitor myocarditis. *JACC Cardiovasc Imaging* 2022;**15**:1883–96.
163. Cadour F, Cautela J, Rapacchi S, Varoquaux A, Habert P, Arnaud F *et al.* Cardiac MRI features and prognostic value in immune checkpoint inhibitor-induced myocarditis. *Radiology* 2022;**303**:512–21.
164. Zhang L, Awadalla M, Mahmood SS, Nohria A, Hassan MZO, Thuny F *et al.* Cardiovascular magnetic resonance in immune checkpoint inhibitor-associated myocarditis. *Eur Heart J* 2020;**41**:1733–43.
165. Chen W, Jeudy J. Assessment of myocarditis: cardiac MR, PET/CT, or PET/MR? *Curr Cardiol Rep* 2019;**21**:76.
166. Palmisano A, Vignale D, Peretto G, Busnardo E, Calcagno C, Campochiaro C *et al.* Hybrid FDG-PET/MR or FDG-PET/CT to detect disease activity in patients with persisting arrhythmias after myocarditis. *JACC Cardiovasc Imaging* 2021;**14**:288–92.
167. Krumm P, Brendel JM, Klingel K, Müller KAL, Kübler J, Gräni C *et al.* Using multiparametric cardiac magnetic resonance to phenotype and differentiate biopsy-proven chronic from healed myocarditis and dilated cardiomyopathy. *J Clin Med* 2022;**11**: 5047.
168. Lurz P, Luecke C, Eitel I, Föhrenbach F, Frank C, Grothoff M *et al.* Comprehensive cardiac magnetic resonance imaging in patients with suspected myocarditis: the MyoRacer-Trial. *J Am Coll Cardiol* 2016;**67**:1800–11.
169. Tanimura M, Dohi K, Imanaka-Yoshida K, Omori T, Moriwaki K, Nakamori S *et al.* Fulminant myocarditis with prolonged active lymphocytic infiltration after hemodynamic recovery. *Int Heart J* 2017;**58**:294–7.
170. Abgral R, Dweck MR, Trivieri MG, Robson PM, Karakatsanis N, Mani V *et al.* Clinical utility of combined FDG-PET/MR to assess myocardial disease. *JACC Cardiovasc Imaging* 2017;**10**:594–7.
171. Nensa F, Tezgah E, Poeppel TD, Jensen CJ, Schelhorn J, Köhler J *et al.* Integrated 18F-FDG PET/MR imaging in the assessment of cardiac masses: a pilot study. *J Nucl Med* 2015;**56**:255–60.
172. Hanneman K, Kadoch M, Guo HH, Jamali M, Quon A, Iagaru A *et al.* Initial experience with simultaneous 18F-FDG PET/MRI in the evaluation of cardiac sarcoidosis and myocarditis. *Clin Nucl Med* 2017;**42**:e328–e34.
173. Upshaw JN, Finkelman B, Hubbard RA, Smith AM, Narayan HK, Arndt L *et al.* Comprehensive assessment of changes in left ventricular diastolic function with contemporary breast cancer therapy. *JACC Cardiovasc Imaging* 2020;**13**:198–210.
174. Border WL, Sachdeva R, Stratton KL, Armenian SH, Bhat A, Cox DE *et al.* Longitudinal changes in echocardiographic parameters of cardiac function in pediatric cancer survivors. *JACC CardioOncol* 2020;**2**:26–37.
175. Mincu RI, Lampe LF, Mahabadi AA, Kimmig R, Rassaf T, Totzeck M. Left ventricular diastolic function following anthracycline-based chemotherapy in patients with breast cancer without previous cardiac disease—a meta-analysis. *J Clin Med* 2021;**10**:3890.
176. Lee BH, Goodenday LS, Muswick GJ, Yasnoff WA, Leighton RF, Skeel RT. Alterations in left ventricular diastolic function with doxorubicin therapy. *J Am Coll Cardiol* 1987;**9**: 184–8.
177. Klein R, Nadouri D, Osler E, Johnson C, Dent S, Dwivedi G. Diastolic dysfunction can precede systolic dysfunction on MUGA in cancer patients receiving trastuzumab-based therapy. *Nucl Med Commun* 2019;**40**:22–9.
178. Aggarwal A, Brown KA, LeWinter MM. Diastolic dysfunction: pathophysiology, clinical features, and assessment with radionuclide methods. *J Nucl Cardiol* 2001;**8**:98–106.
179. Reuvekamp EJ, Bulten BF, Nieuwenhuis AA, Meekes MR, de Haan AF, Tol J *et al.* Does diastolic dysfunction precede systolic dysfunction in trastuzumab-induced cardiotoxicity? Assessment with multigated radionuclide angiography (MUGA). *J Nucl Cardiol* 2016;**23**:824–32.
180. Hansen NL, Haarmark C, Zerahn B. Ventricular peak emptying and filling rates measured by gated tomographic radionuclide angiography using a cadmium-zinc-telluride SPECT camera in chemotherapy-naïve cancer patients. *J Nucl Cardiol* 2020;**27**: 1193–201.
181. Chamsi-Pasha MA, Zhan Y, Debs D, Shah DJ. CMR in the evaluation of diastolic dysfunction and phenotyping of HFpEF: current role and future perspectives. *JACC Cardiovasc Imaging* 2020;**13**:283–96.
182. Slart R, Tio RA, Elsinga PH, Schwaiger M. *Autonomic Innervation of the Heart*. New York City: Springer Publishing; 2015. p235–53.
183. Zelt JGE, deKemp RA, Rotstein BH, Nair GM, Narula J, Ahmadi A *et al.* Nuclear imaging of the cardiac sympathetic nervous system: a disease-specific interpretation in heart failure. *JACC Cardiovasc Imaging* 2020;**13**:1036–54.
184. Laursen AH, Thune JJ, Hutchings M, Hasbak P, Kjaer A, Elming MB *et al.* (123) I-MIBG imaging for detection of anthracycline-induced cardiomyopathy. *Clin Physiol Funct Imaging* 2018;**38**:176–85.
185. Gimelli A, Liga R, Agostini D, Bengel FM, Ernst S, Hyafil F *et al.* The role of myocardial innervation imaging in different clinical scenarios: an expert document of the European Association of Cardiovascular Imaging and Cardiovascular Committee of the European Association of Nuclear Medicine. *Eur Heart J Cardiovasc Imaging* 2021;**22**: 480–90.
186. Santos MJ D, da Rocha ET, Verberne HJ, da Silva ET, Aragon DC, Junior JS. Assessment of late anthracycline-induced cardiotoxicity by (123)I-mIBG cardiac scintigraphy in patients treated during childhood and adolescence. *J Nucl Cardiol* 2017;**24**:256–64.
187. Lekakis J, Prassopoulos V, Athanassiadis P, Kostamis P, Moulopoulos S. Doxorubicin-induced cardiac neurotoxicity: study with iodine 123-labeled metaiodobenzylguanidine scintigraphy. *J Nucl Cardiol* 1996;**3**:37–41.
188. Arrais TR, Cavalli GD, Dos Santos BT, Pereira GB, Migliavaca CB, Grossman GB *et al.* MIBG cardiac imaging compared to ejection fraction in evaluation of cardiotoxicity: a systematic review. *J Nucl Cardiol* 2021;**29**:2274–91.
189. Carrió I, Estorch M, Berná L, López-Pousa J, Tabernero J, Torres G. Indium-111-antimyosin and iodine-123-MIBG studies in early assessment of doxorubicin cardiotoxicity. *J Nucl Med* 1995;**36**:2044–9.
190. Valdés Olmos RA, ten Bokkel Huinink WW, ten Hoeve RF, van Tinteren H, Bruning PF, van Vlies B *et al.* Assessment of anthracycline-related myocardial adrenergic derangement by [123I]metaiodobenzylguanidine scintigraphy. *Eur J Cancer* 1995;**31a**:26–31.
191. Kelly JM, Babich JW. PET tracers for imaging cardiac function in cardio-oncology. *Curr Cardiol Rep* 2022;**24**:247–60.
192. Burger IA, Lohmann C, Messerli M, Bengs S, Becker A, Maredziak M *et al.* Age- and sex-dependent changes in sympathetic activity of the left ventricular apex assessed by 18F-DOPA PET imaging. *PLoS One* 2018;**13**:e0202302.
193. Bozkurt MF, Virgolini I, Balogova S, Beheshti M, Rubello D, Decristoforo C *et al.* Guideline for PET/CT imaging of neuroendocrine neoplasms with (68) Ga-DOTA-conjugated somatostatin receptor targeting peptides and (18)F-DOPA. *Eur J Nucl Med Mol Imaging* 2017;**44**:1588–601.
194. Wang JZ, Moody JB, Kaps N, Britt D, Lavallee A, Renaud JM *et al.* Reproducible quantification of regional sympathetic denervation with [(11)C]meta-hydroxyephedrine PET imaging. *J Nucl Cardiol* 2021c;**28**:2745–57.
195. Lopaschuk GD, Karwi QG, Tian R, Wende AR, Abel ED. Cardiac energy metabolism in heart failure. *Circ Res* 2021;**128**:1487–513.
196. Bertero E, Maack C. Metabolic remodelling in heart failure. *Nat Rev Cardiol* 2018;**15**: 457–70.
197. Peterson LR, Gropler RJ. Radionuclide imaging of myocardial metabolism. *Circ Cardiovasc Imaging* 2010;**3**:211–22.
198. Tong D, Zaha VG. Metabolic imaging in cardio-oncology. *J Cardiovasc Transl Res* 2020; **13**:357–66.
199. Yoshinaga K, Tamaki N. Current status of nuclear cardiology in Japan: ongoing efforts to improve clinical standards and to establish evidence. *J Nucl Cardiol* 2015;**22**:690–9.
200. Saito K, Takeda K, Imanaka-Yoshida K, Imai H, Sekine T, Kamikura Y. Assessment of fatty acid metabolism in taxan-induced myocardial damage with iodine-123 BMIPP

SPECT: comparative study with myocardial perfusion, left ventricular function, and histopathological findings. *Ann Nucl Med* 2003;**17**:481–8.
201. Cho SG, Kim YH, Park H, Park KS, Kim J, Ahn SJ *et al.* Prediction of cardiac events following concurrent chemoradiation therapy for non-small-cell lung cancer using FDG PET. *Ann Nucl Med* 2022;**36**:439–49.
202. Kim J, Cho SG, Kang SR, Yoo SW, Kwon SY, Min JJ *et al.* Association between FDG uptake in the right ventricular myocardium and cancer therapy-induced cardiotoxicity. *J Nucl Cardiol* 2020;**27**:2154–63.
203. Jingu K, Kaneta T, Nemoto K, Ichinose A, Oikawa M, Takai Y *et al.* The utility of 18F-fluorodeoxyglucose positron emission tomography for early diagnosis of radiation-induced myocardial damage. *Int J Radiat Oncol Biol Phys* 2006;**66**:845–51.
204. Unal K, Unlu M, Akdemir O, Akmansu M. 18F-FDG PET/CT findings of radiotherapy-related myocardial changes in patients with thoracic malignancies. *Nucl Med Commun* 2013;**34**:855–9.
205. Evans JD, Gomez DR, Chang JY, Gladish GW, Erasmus JJ, Rebueno N *et al.* Cardiac ^{18}F-fluorodeoxyglucose uptake on positron emission tomography after thoracic stereotactic body radiation therapy. *Radiother Oncol* 2013;**109**:82–8.
206. Jo IY, Lee JW, Kim WC, Min CK, Kim ES, Yeo SG *et al.* Relationship between changes in myocardial F-18 fluorodeoxyglucose uptake and radiation dose after adjuvant three-dimensional conformal radiotherapy in patients with breast cancer. *J Clin Med* 2020; **9**:666.
207. Haider A, Bengs S, Schade K, Wijnen WJ, Portmann A, Etter D *et al.* Myocardial (18) F-FDG uptake pattern for cardiovascular risk stratification in patients undergoing oncologic PET/CT. *J Clin Med* 2020;**9**:2279.
208. Osborne MT, Hulten EA, Murthy VL, Skali H, Taqueti VR, Dorbala S *et al.* Patient preparation for cardiac fluorine-18 fluorodeoxyglucose positron emission tomography imaging of inflammation. *J Nucl Cardiol* 2017;**24**:86–99.
209. Ishida Y, Sakanaka K, Itasaka S, Nakamoto Y, Togashi K, Mizowaki T *et al.* Effect of long fasting on myocardial accumulation in 18F-fluorodeoxyglucose positron emission tomography after chemoradiotherapy for esophageal carcinoma. *J Radiat Res* 2018;**59**: 182–9.
210. Zampella E, Assante R, Acampa W, Gaudieri V, Nappi C, Mannarino T *et al.* Incremental value of (18)F-FDG cardiac PET imaging over dobutamine stress echocardiography in predicting myocardial ischemia in patients with suspected coronary artery disease. *J Nucl Cardiol* 2022;**29**:3028–38.
211. Yoshii Y, Furukawa T, Saga T, Fujibayashi Y. Acetate/acetyl-CoA metabolism associated with cancer fatty acid synthesis: overview and application. *Cancer Lett* 2015; **356**:211–6.
212. Wu KY, Dinculescu V, Renaud JM, Chen SY, Burwash IG, Mielniczuk LM *et al.* Repeatable and reproducible measurements of myocardial oxidative metabolism, blood flow and external efficiency using (11)C-acetate PET. *J Nucl Cardiol* 2018;**25**: 1912–25.
213. O'Farrell AC, Evans R, Silvola JM, Miller IS, Conroy E, Hector S *et al.* A novel positron emission tomography (PET) approach to monitor cardiac metabolic pathway remodeling in response to sunitinib malate. *PLoS One* 2017;**12**:e0169964.
214. Boutagy NE, Wu J, Cai Z, Zhang W, Booth CJ, Kyriakides TC *et al.* In vivo reactive oxygen species detection with a novel positron emission tomography tracer, (18) F-DHMT, allows for early detection of anthracycline-induced cardiotoxicity in rodents. *JACC Basic Transl Sci* 2018;**3**:378–90.
215. Mota F, Pell VR, Singh N, Baark F, Waters E, Sadasivam P *et al.* A reactivity-based (18) F-labeled probe for PET imaging of oxidative stress in chemotherapy-induced cardiotoxicity. *Mol Pharm* 2022;**19**:18–25.
216. Detmer FJ, Alpert NM, Moon SH, Dhaynaut M, Guerrero JL, Guehl NJ *et al.* PET imaging of mitochondrial function in acute doxorubicin-induced cardiotoxicity: a proof-of-principle study. *Sci Rep* 2022;**12**:6122.
217. Thackeray JT, Hupe HC, Wang Y, Bankstahl JP, Berding G, Ross TL *et al.* Myocardial inflammation predicts remodeling and neuroinflammation after myocardial infarction. *J Am Coll Cardiol* 2018;**71**:263–75.
218. Wang X, Feng H, Zhao S, Xu J, Wu X, Cui J *et al.* SPECT And PET radiopharmaceuticals for molecular imaging of apoptosis: from bench to clinic. *Oncotarget* 2017;**8**:20476–95.
219. Benali K, Louedec L, Azzouna RB, Merceron O, Nassar P, Al Shoukr F *et al.* Preclinical validation of 99mTc-annexin A5-128 in experimental autoimmune myocarditis and infective endocarditis: comparison with 99mTc-HYNIC-annexin A5. *Mol Imaging* 2014:13. doi: 10.2310/7290.2014.00049.
220. Gabrielson KL, Mok GS, Nimmagadda S, Bedja D, Pin S, Tsao A *et al.* Detection of dose response in chronic doxorubicin-mediated cell death with cardiac technetium 99m annexin V single-photon emission computed tomography. *Mol Imaging* 2008;**7**:132–8.
221. Van de Wiele C, Ustmert S, De Spiegeleer B, De Jonghe PJ, Sathekge M, Alex M. Apoptosis imaging in oncology by means of positron emission tomography: a review. *Int J Mol Sci* 2021;**22**:2753.
222. Su H, Chen G, Gangadharmath U, Gomez LF, Liang Q, Mu F *et al.* Evaluation of [(18) F]-CP18 as a PET imaging tracer for apoptosis. *Mol Imaging Biol* 2013;**15**:739–47.
223. Su H, Gorodny N, Gomez LF, Gangadharmath U, Mu F, Chen G *et al.* Noninvasive molecular imaging of apoptosis in a mouse model of anthracycline-induced cardiotoxicity. *Circ Cardiovasc Imaging* 2015;**8**:e001952.
224. Carrió I, Lopez-Pousa A, Estorch M, Duncker D, Berná L, Torres G *et al.* Detection of doxorubicin cardiotoxicity in patients with sarcomas by indium-111-antimyosin monoclonal antibody studies. *J Nucl Med* 1993;**34**:1503–7.
225. Estorch M, Carrió I, Berná L, Martínez-Duncker C, Alonso C, Germá JR *et al.* Indium-111-antimyosin scintigraphy after doxorubicin therapy in patients with advanced breast cancer. *J Nucl Med* 1990;**31**:1965–9.
226. Francis Stuart SD, De Jesus NM, Lindsey ML, Ripplinger CM. The crossroads of inflammation, fibrosis, and arrhythmia following myocardial infarction. *J Mol Cell Cardiol* 2016; **91**:114–22.
227. Tadic M, Cuspidi C, Marwick TH. Phenotyping the hypertensive heart. *Eur Heart J* 2022;**43**:3794–810.
228. Hassan S, Barrett CJ, Crossman DJ. Imaging tools for assessment of myocardial fibrosis in humans: the need for greater detail. *Biophys Rev* 2020;**12**:969–87.
229. Nagaraju CK, Dries E, Popovic N, Singh AA, Haemers P, Roderick HL *et al.* Global fibroblast activation throughout the left ventricle but localized fibrosis after myocardial infarction. *Sci Rep* 2017;**7**:10801.
230. Varasteh Z, Mohanta S, Robu S, Braeuer M, Li Y, Omidvari N *et al.* Molecular imaging of fibroblast activity after myocardial infarction using a (68)Ga-labeled fibroblast activation protein inhibitor, FAPI-04. *J Nucl Med* 2019;**60**:1743–9.
231. Qiao P, Wang Y, Zhu K, Zheng D, Song Y, Jiang D *et al.* Noninvasive monitoring of reparative fibrosis after myocardial infarction in rats using (68)Ga-FAPI-04 PET/CT. *Mol Pharm* 2022;**19**:4171–8.
232. Song W, Zhang X, He S, Gai Y, Qin C, Hu F *et al.* (68)Ga-FAPI PET visualize heart failure: from mechanism to clinic. *Eur J Nucl Med Mol Imaging* 2023;**50**:475–85.
233. Zhu W, Guo F, Wang Y, Ding H, Huo L. 68Ga-FAPI-04 accumulation in myocardial infarction in a patient with neuroendocrine carcinoma. *Clin Nucl Med* 2020;**45**:1020–2.
234. Heckmann MB, Reinhardt F, Finke D, Katus HA, Haberkorn U, Leuschner F *et al.* Relationship between cardiac fibroblast activation protein activity by positron emission tomography and cardiovascular disease. *Circ Cardiovasc Imaging* 2020;**13**:e010628.
235. Wei Y, Sun Y, Liu J, Zhang G, Qin X, Xu S *et al.* Early detection of radiation-induced myocardial damage by [(18)F]AlF-NOTA-FAPI-04 PET/CT imaging. *Eur J Nucl Med Mol Imaging* 2023;**50**:453–64.
236. Kim DY, Park MS, Youn JC, Lee S, Choi JH, Jung MH *et al.* Development and validation of a risk score model for predicting the cardiovascular outcomes after breast cancer therapy: the CHEMO-RADIAT score. *J Am Heart Assoc* 2021;**10**:e021931.
237. Ezaz G, Long JB, Gross CP, Chen J. Risk prediction model for heart failure and cardiomyopathy after adjuvant trastuzumab therapy for breast cancer. *J Am Heart Assoc* 2014;**3**:e000472.
238. Muehlberg F, Funk S, Zange L, von Knobelsdorff-Brenkenhoff F, Blaszczyk E, Schulz A *et al.* Native myocardial T1 time can predict development of subsequent anthracycline-induced cardiomyopathy. *ESC Heart Fail* 2018;**5**:620–9.
239. Cheung E, Ahmad S, Aitken M, Chan R, Iwanochko RM, Balter M *et al.* Combined simultaneous FDG-PET/MRI with T1 and T2 mapping as an imaging biomarker for the diagnosis and prognosis of suspected cardiac sarcoidosis. *Eur J Hybrid Imaging* 2021; **5**:24.
240. Kwan JM, Oikonomou EK, Henry ML, Sinusas AJ. Multimodality advanced cardiovascular and molecular imaging for early detection and monitoring of cancer therapy-associated cardiotoxicity and the role of artificial intelligence and big data. *Front Cardiovasc Med* 2022;**9**:829553.
241. Madan N, Lucas J, Akhter N, Collier P, Cheng F, Guha A *et al.* Artificial intelligence and imaging: opportunities in cardio-oncology. *Am Heart J Plus* 2022;**15**:100126.
242. Betancur J, Otaki Y, Motwani M, Fish MB, Lemley M, Dey D *et al.* Prognostic value of combined clinical and myocardial perfusion imaging data using machine learning. *JACC Cardiovasc Imaging* 2018;**11**:1000–9.
243. Zhu Y, Li H, Guo W, Drukker K, Lan L, Giger ML *et al.* Deciphering genomic underpinnings of quantitative MRI-based radiomic phenotypes of invasive breast carcinoma. *Sci Rep* 2015;**5**:17787.
244. Young JD, Cai C, Lu X. Unsupervised deep learning reveals prognostically relevant subtypes of glioblastoma. *BMC Bioinformatics* 2017;**18**:381.
245. Grossmann P, Stringfield O, El-Hachem N, Bui MM, Rios Velazquez E, Parmar C *et al.* Defining the biological basis of radiomic phenotypes in lung cancer. *Elife* 2017;**6**: e23421.
246. Dreyfuss AD, Bravo PE, Koumenis C, Ky B. Precision cardio-oncology. *J Nucl Med* 2019;**60**:443–50.
247. Park S, Parihar AS, Bodei L, Hope TA, Mallak N, Millo C *et al.* Somatostatin receptor imaging and theranostics: current practice and future prospects. *J Nucl Med* 2021;**62**: 1323–9.
248. Perik PJ, Lub-De Hooge MN, Gietema JA, van der Graaf WT, de Korte MA, Jonkman S *et al.* Indium-111-labeled trastuzumab scintigraphy in patients with human epidermal growth factor receptor 2-positive metastatic breast cancer. *J Clin Oncol* 2006;**24**: 2276–82.